**Zeitschrift:** Schweizerische mineralogische und petrographische Mitteilungen =

Bulletin suisse de minéralogie et pétrographie

**Band:** 75 (1995)

Heft: 1

**Artikel:** Teritary Himalayan structures and metamorphism in the Kulu Valley

(Mandi-Khoksar transect of the Western Himalaya) - Shikar Beh Nappe

and Crystalline Nappe

Autor: Epard, Jean-Luc / Steck, Albrecht / Vannay, Jean-Claude

**DOI:** https://doi.org/10.5169/seals-57144

### Nutzungsbedingungen

Die ETH-Bibliothek ist die Anbieterin der digitalisierten Zeitschriften auf E-Periodica. Sie besitzt keine Urheberrechte an den Zeitschriften und ist nicht verantwortlich für deren Inhalte. Die Rechte liegen in der Regel bei den Herausgebern beziehungsweise den externen Rechteinhabern. Das Veröffentlichen von Bildern in Print- und Online-Publikationen sowie auf Social Media-Kanälen oder Webseiten ist nur mit vorheriger Genehmigung der Rechteinhaber erlaubt. Mehr erfahren

#### **Conditions d'utilisation**

L'ETH Library est le fournisseur des revues numérisées. Elle ne détient aucun droit d'auteur sur les revues et n'est pas responsable de leur contenu. En règle générale, les droits sont détenus par les éditeurs ou les détenteurs de droits externes. La reproduction d'images dans des publications imprimées ou en ligne ainsi que sur des canaux de médias sociaux ou des sites web n'est autorisée qu'avec l'accord préalable des détenteurs des droits. En savoir plus

#### Terms of use

The ETH Library is the provider of the digitised journals. It does not own any copyrights to the journals and is not responsible for their content. The rights usually lie with the publishers or the external rights holders. Publishing images in print and online publications, as well as on social media channels or websites, is only permitted with the prior consent of the rights holders. Find out more

**Download PDF:** 03.12.2025

ETH-Bibliothek Zürich, E-Periodica, https://www.e-periodica.ch

# Tertiary Himalayan structures and metamorphism in the Kulu Valley (Mandi–Khoksar transect of the Western Himalaya) – Shikar Beh Nappe and Crystalline Nappe

by Jean-Luc Epard<sup>1</sup>, Albrecht Steck<sup>1</sup>, Jean-Claude Vannay<sup>1</sup> and Johannes Hunziker<sup>1</sup>

#### **Abstract**

The Crystalline Nappe of the High Himalayan Crystalline has been examined along the Kulu Valley and its vicinity (Mandi–Khoksar transect). This nappe was believed to have undergone deformation related only to its transport towards the SW essentially during the "Main Central Thrust event". New data has led to the conclusion that during the Himalayan orogeny, two distinctive phases, related to two opposite transport directions, characterize the evolution of this part of the chain, before the creation of the late NE-vergent backfolding.

The first phase corresponds to an early NE-vergent folding and thrusting, creating the Tandi Syncline and the NE-oriented Shikar Beh Nappe stack, with a displacement amplitude of about 50 km. Two schistosities, together with a strong stretching lineation are developed at a deep tectonic level under amphibolite facies conditions (kyanite-staurolite-garnet-two mica schists). At a higher tectonic level and in the southern part of the section (Tandy Syncline and southern Kulu Valley between Kulu and Mandi) one or two schistosities are developed in the greenschist facies grade rocks (garnet-biotite and biotite schists). These structures and the associated Barrovian type metamorphism are all related to the NE-verging Shikar Beh Nappe. The creation of the NE-verging Shikar Beh Nappe may be explained by the reactivation of a SW dipping listric normal fault of the N Indian flexural passive margin, during the early stages of the Himalayan orogeny.

In the second phase, the still hot metamorphic rocks of the Shikar Beh Nappe were folded and thrust towards the SW (mainly along the MBT and the MCT with a displacement in excess of 100 km) onto the cold, low-grade metamorphic rocks of the Larji-Kulu-Rampur Window or, near Mandi, on the non-metamorphic sandstones of the Ganges Molasse (Siwaliks). Sense of shear criteria and a strong NE–SW stretching-lineation indicate that the Crystalline Nappe has been overthrusted towards the SW. Thermometry on synkinematically crystallised garnet-biotite and garnet-hornblende pairs reveals the lower amphibolite facies temperature conditions related to the Crystalline Nappe formation.

From the muscovite and biotite Rb-Sr cooling ages, the Shikar Beh Nappe emplacement occurred before 32 Ma and the southwestward thrusting of the Crystalline Nappe began before 21 Ma. Our model involving two opposite directions of thrusting goes against the conventional idea of only one main SW-oriented transport direction in the High Himalayan Crystalline Nappes.

Keywords: Himalaya, Himachal Pradesh, Crystalline Nappe, Main Central Thrust, tectonics, metamorphism, thermo-barometry.

#### Introduction

The Kulu Valley offers a continuous geological section through the southern part of the Himalayan chain (Figs 1 and 2). The Tertiary sandstones of the Siwaliks (Ganges Molasse) are exposed south of Mandi. At Mandi, these unmetamorphosed Molasse sediments are overthrusted along the Main Boundary Thrust (MBT), by two thin tec-

tonic units (the Mandi Unit and the Bajaura Nappe). Some 5 km farther to the NE, the Main Central Thrust (MCT) places the greenschist facies metamorphic sediments of the Crystalline Nappe onto the Bajaura Nappe (Frank et al., 1973, 1977a; Mehta, 1977; Le Fort, 1986). The Crystalline Nappe is composed by metamorphosed graywackes of Proterozoic to Cambrian age (Phe Formation or Haimantas), intruded by

<sup>&</sup>lt;sup>1</sup> Instituts de Minéralogie et de Géologie, Université de Lausanne, BFSH2, CH-1015 Lausanne, Switzerland.

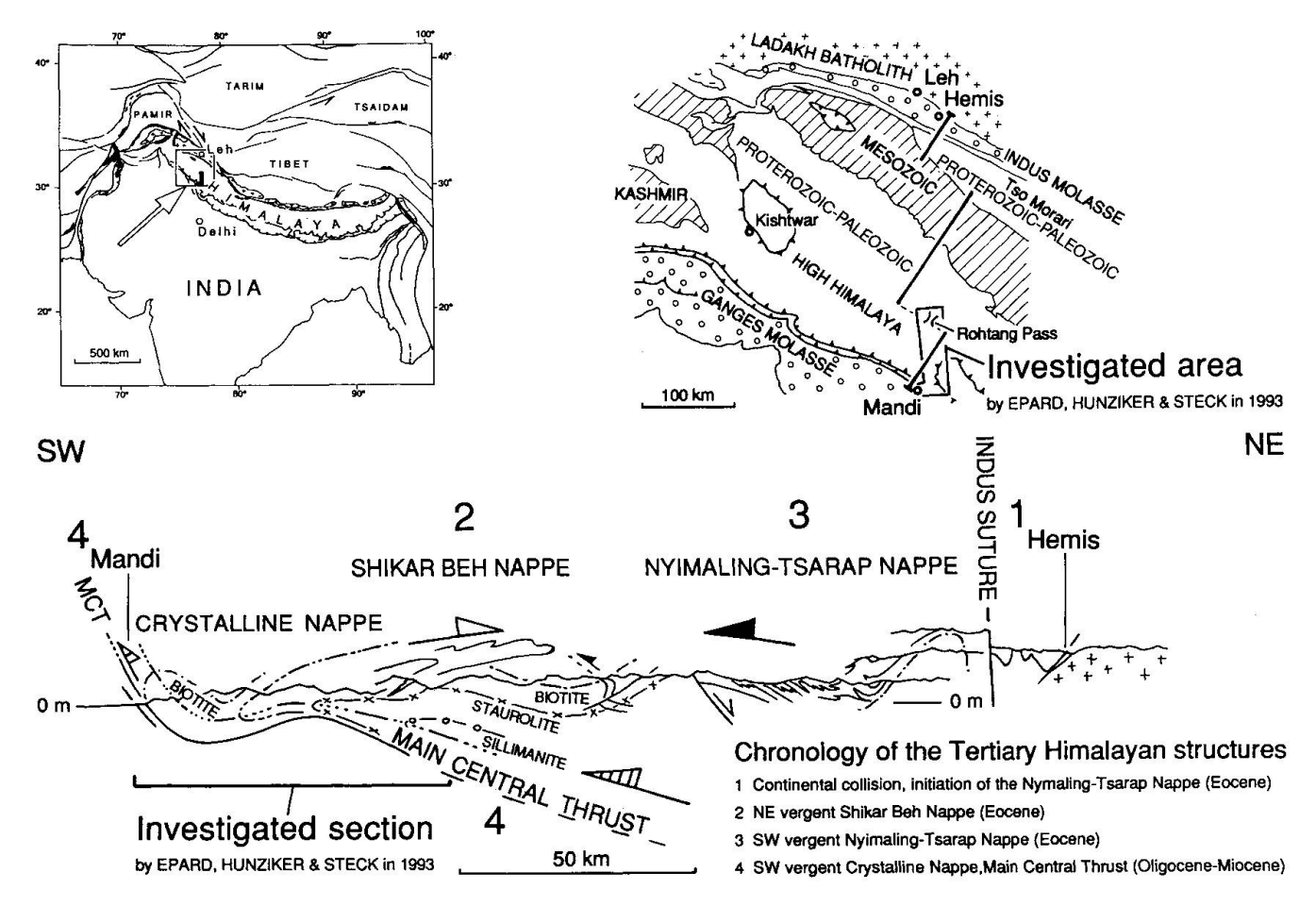


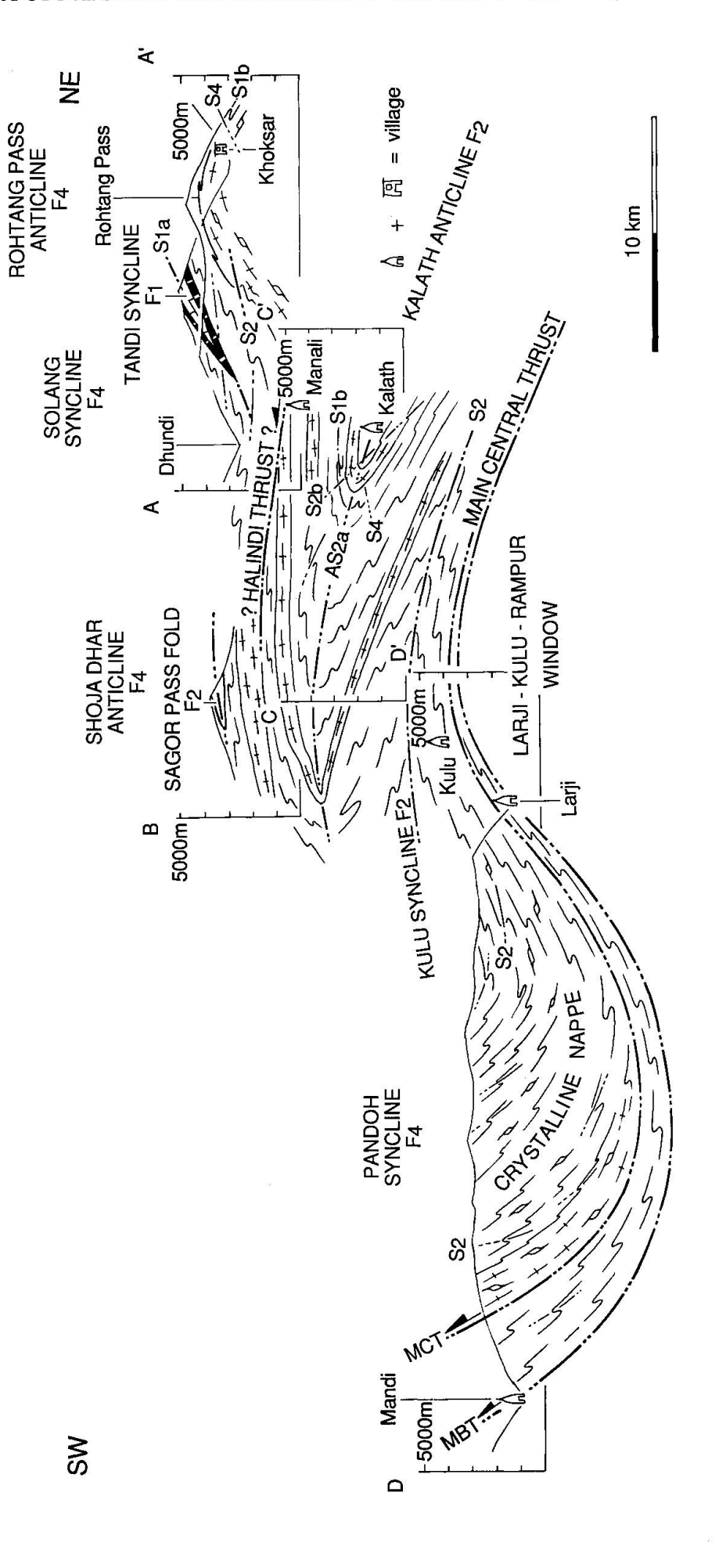
Fig. 1 Index map of the investigated area in Himachal Pradesh and cross section of the Western Himalaya, after STECK et al. (1993 a and b).

granites of Cambro-Ordovician ages. West of the Rohtang Pass and in the Chandra and Chenab Valleys south of Tandi, the graywackes of the Phe Formation are stratigraphically overlain by the Triassic and Jurassic limestones, Permian. dolomites and marls of the Tandi Syncline. Silurian sandstones, Carboniferous limestones and Permo-Mesozoic sediments are also exposed on top of the Phe Formation south of the Baralacha La and east of the upper Chandra Valley. The rocks of the Larji-Kulu-Rampur tectonic window, situated below the Crystalline Nappe, consist of very low grade metamorphic, mainly Proterozoic, sediments and metagranites. The thin Bajaura Nappe separates the Crystalline Nappe from the Larji-Kulu-Rampur sequence in this area.

The region where the metamorphic rocks of the Crystalline Nappe outcrop at up to 6000 m in elevation is called the Higher Himalaya or the High Himalayan Crystalline. The Bajaura Nappe and the Larji-Kulu-Rampur sequences belong to the Lesser Himalaya (Frank et al., 1973, 1977a, 1987, 1992; Powell and Conaghan, 1973 and 1978; Srikantia and Bhargava, 1979, 1982; Thö-

NI, 1977; MEHTA, 1977, 1978; STECK et al., 1993 a and b; Vannay, 1993; Vannay and STECK, in press).

The following tectono-metamorphic model for the evolution of the Crystalline Nappe is consistent with published data from other authors. The regional metamorphism with biotite-, garnet-, kyanite-, kyanite-staurolite- and sillimanitezones in pelitic rocks is of Barrovian type and of a Cenozoic age (Frank et al., 1973, 1977a; Thöni, 1977). The thermal peak of this metamorphism occurred before 32 Ma as deduced from Rb-Sr muscovite cooling ages of 32 ± 2 Ma (Frank et al., 1977a). Frank et al. (1973) proposed the existence of an abnormally high geothermal gradient of 37-45° C/km to explain the presence of amphibolite grade rocks (staurolite zone) in the Khoksar region. This conclusion is based on the observation that the thickness of the stratigraphic series responsible for the overburden does not exceed 12-15 km. The main thrusting to the SW of the Crystalline Nappe is younger than the peak of metamorphism. It occurred during a period of retrograde crystallisation. The spectacular SW-verging Kalath fold in the Crystalline Nappe deforms the pre-existing isograde surfaces (Thöni, 1977). The



Structural section between Mandi in the Kulu Valley and Khoksar in the Chandra Valley (locations of sections A-A', B-B', C-C' and D-D' on Fig. 10). Fig. 2

folding and thrusting of the hot rocks of the Crystalline Nappe onto the cold rocks exposed in the Kulu-Larji-Rampur Window caused the inverted metamorphic zonation in this area.

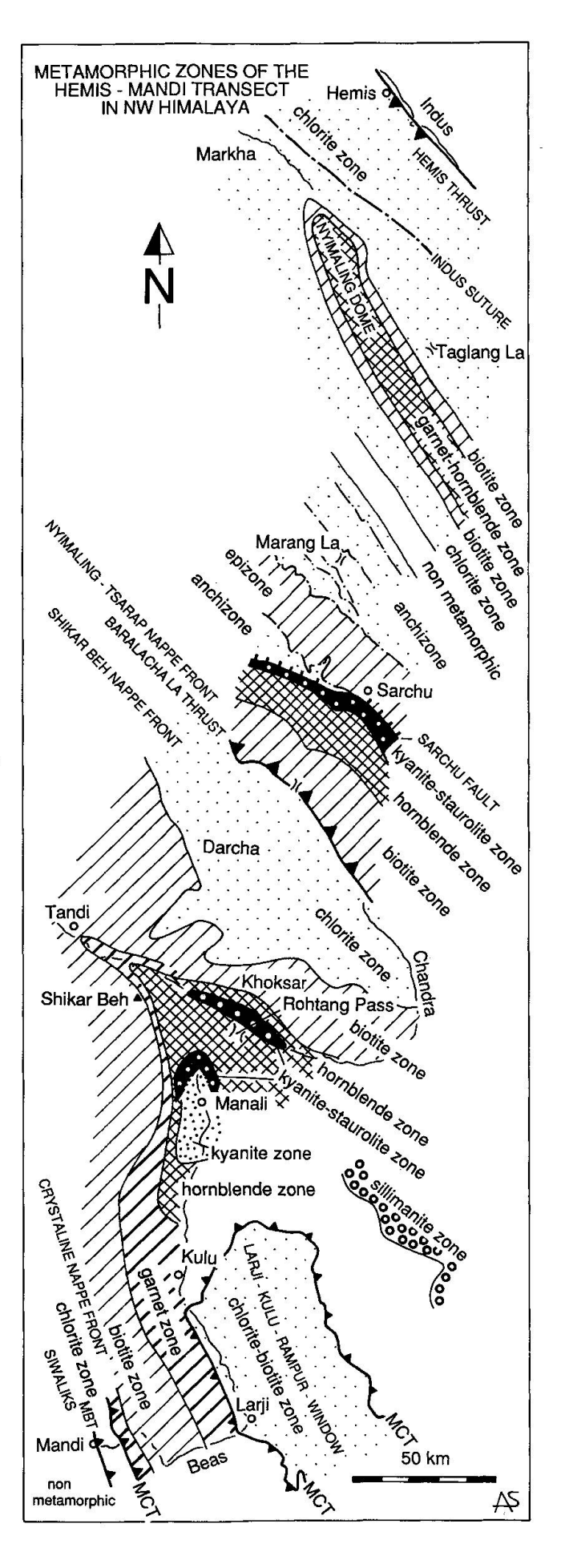
Since 1979, members of Lausanne University have been working on a geological transect of the NW Himalaya located between Hemis and Leh in the upper Indus Valley to the N, and Mandi on the Main Boundary Thrust and the Siwaliks (Ganges Molasse) to the S (BAUD et al., 1982, 1984; STUTZ and STECK, 1986; STUTZ, 1988; SPRING and Crespo-Blanc, 1992; Spring, 1993; Spring et al., 1993 a and b; VANNAY, 1993; VANNAY and Spring, 1993). The main results of the different expeditions are summarized and compiled in STECK et al. (1993 a and b). This synthesis is also based on observations by GANSSER (1964 and 1981), Fuchs (1982, 1987, 1992), Frank et al. (1977 a and b), GAETANI et al. (1986), GAETANI and Garzanti (1991), Honegger (1983), Honeg-GER et al. (1982), KÜNDIG (1988 and 1989).

Our investigations corroborate the main conclusions of the Vienna group (Frank, Grasemann, Thöni and collaborators) mainly that:

- the Crystalline Nappe represents the product of a multiphase structural and metamorphic evolution (STECK et al., 1993 a and b; VANNAY, 1993; VANNAY and STECK, in press);
- the deformational structures and the growth of the metamorphic minerals are all younger than the Palaeozoic and Mesozoic sediments of the Tandi Syncline. These structures are therefore related to Himalayan tectonic events;
- the peak of the Barrovian type metamorphism is related to a group of early Cenozoic structures. The products of this early tectonometamorphic phase are overprinted by a regional retrograde metamorphism, which is synkinematic with the formation of late schistosities, stretching lineations and folds. This second tectono-metamorphic phase is related to the Crystalline Nappe formation.

Our interpretation for the early Himalayan tectono-metamorphic process responsible for the Paleogene Barrovian metamorphism differs from those given by the previous authors. The proposed high geothermal gradient of 37–45 °C/km for the early phase of Barrovian metamorphism (Frank et al., 1973) is questionable. From our observations and constructions (Steck et al., 1993)

Fig. 3 Zonation of the Tertiary metamorphism of the Hemis-Mandi transect in the Western Himalaya (after Frank et al., 1977a; Thöni, 1977; Stutz, 1988; Spring, 1993; Steck et al., 1993 a and b; Vannay, 1993 and this study).



a and b), the initial stratigraphic overburden above the staurolite zone of the Chandra Valley was less than 10 km, considerably shallower than the 12-15 km of Frank et al. (1973). Under these conditions, the geothermal gradient for this overburden would be of about 55 °C/km. This is the geothermal gradient of a Buchan-type (andalusite-sillimanite) metamorphism. We propose that the geothermal gradient responsible for the Barrovian-type metamorphism was approximately 20-30 °C/km, and that the overburden responsible for the staurolite zone is of tectonic origin. Additionally, there is the problem of the tectonic significance of the NE-verging Tandi Syncline situated on the top of the SW-verging Crystalline Nappe. Therefore, we aim to answer three main questions:

- What is the tectonic mechanism responsible for the Barrovian regional metamorphism that extends over 90 km from the Baralacha La to the N to the southwestern front of the Crystalline nappe?
- What is the tectonic significance of the NEverging Tandi Syncline and of related deformational structures?
- What are the structures and metamorphism related to the Crystalline Nappe?

In order to answer these questions, STECK et al. (1993 a and b) and VANNAY (1993) subdivided the tectonic evolution of the High Himalayan Crystalline into two main events: the Eocene thrusting of a nappe stack (the Shikar Beh Nappe) towards the NE and the Miocene emplacement of the Crystalline Nappe towards the SW. The Shikar Beh Nappe is named after the highest mountain peak in this region, situated in the lowest part of the Shikar Beh Nappe stack.

The NE-vergence of the Tandi Syncline (Fig. 2) together with the regional metamorphism distribution (Fig. 3) led Steck et al. (1993 a and b), Vannay (1993) and Vannay and Steck (in press) to the conclusion of the existence of a NE-verging Shikar Beh Nappe stack (Fig. 1). This metamorphism reached amphibolite facies conditions in the lower part of the Chandra Valley (kyanitestaurolite zone near Khoksar) and decreases towards the NE to lower greenschist and pumpellyite-actinolite facies just SW of the frontal part of Nyimaling-Tsarap Nappe (chlorite-stilpnomelane-pumpellyite south of the Baralacha La Thrust). The sediments that outcrop along this profile are approximately from the same stratigraphic level. Further north, the metamorphic grade increases again due to the Nyimaling-Tsarap Nappe formation (staurolite-kyanite-garnet in the Sarchu area). The high grade regional metamorphism of the lower part of the Chandra

Valley therefore cannot be related to the Nyimaling-Tsarap Nappe because the two high-grade metamorphic regions are separated by a low grade metamorphic domain. It can only be explained by a stack of nappes thrust from the SW toward the NE and this over a distance of 50 km. The vergence of the Tandi Syncline is in accordance with this movement direction. These observations lead to the conclusion that, in the Chandra and Bhaga Valleys, the Tertiary deformation started with an intracontinental underthrusting of a north-eastern block below a south-western one. This crustal thickening is responsible for the regional metamorphism in the Chandra Valley-Rohtang La region. The total thickness of the Nappe overburden situated on the top of the staurolite-kyanite-garnet assemblage in the Khoksar region and sillimanite-bearing metapelites in the Parbati Valley (THÖNI, 1977; MAR-TIN Wyss, personal communication) was in excess of 20 km and the kyanite-sillimanite type metamorphism indicates a pressure of about 4 to 5 kbar (Richardson et al., 1969).

A new detailed structural and metamorphic analysis of the High Himalayan Crystalline between Mandi and Khoksar was initiated to constrain this hypothesis. The present paper is the result of field data collected by J.-L. Epard, J. Hunziker and A. Steck during a 9 week expedition in the Chandra and Kulu Valleys in the summer of 1993. Detailed structural analysis as well as mineralogical observations were performed in order to provide a better understanding of the structural and metamorphic evolution of the Crystalline Nappe and the High Himalayan Crystalline exposed between Khoksar, the Rohtang Pass and Mandi. Considering our working hypothesis, the distinction between (a) the old structures (folds, schistosities, stretching lineations) and minerals assemblages related to the Shikar Beh Nappe with its high grade metamorphism of Barrovian type and (b) the younger structures and minerals of the Crystalline nappe created during its movement towards the SW under retrograde conditions was made in the field where possible. It was indeed often possible to observe on the outcrop the crystallisation/deformation relationship of biotite, garnet, hornblende, kyanite and staurolite blasts within such structures as folds and schistosities. Additionally, oriented samples collected along the section were analysed in the laboratory to determine the metamorphic mineral paragenesis, the crystallisationdeformation history and the thermo-barometry.

The results of the tectono-metamorphic study conducted along the Kulu Valley transect are presented according to the chronology of the Terti-

Tab. 1 Chronology of the Tertiary Himalayan structures and metamorphism in the Kulu Valley (Mandi-Khoksar transect).

Early NE-verging movements: Tandi Syncline, Shikar Beh Nappe and regional Barrovian metamorphism

- A) First NE-verging  $F_{1a}$ -folds,  $S_{1a}$ -axial surface schistosity and NE-oriented  $L_{1a}$ -stretching lineation
- B) Second NE-verging  $F_{1b}$ -folds,  $S_{1b}$ -axial surface schistosity and NE-oriented  $L_{1b}$ -stretching lineation

Main SW-verging deformations: Crystalline Nappe, Main Central Thrust and synkinematic retrograde metamorphism

C)  $\hat{S}W$ -verging  $F_2$ -folds,  $S_2$ -axial surface schistosity, and NE-oriented  $L_2$ -stretching lineation (in SW-verging Kalath Anticline:  $AS_{2a}$ -axial surface and  $F_{2a}$ -anticline and SW-verging  $F_{2b}$ -folds and  $S_{2b}$ -axial surface schistosity)

Dextral transpression and backfolding

- D) Late dextral shearing in the lower Chandra Valley and Rohtang La region
- E) NE-verging F<sub>4</sub>-"back" folds

Late extensional structures

F) Intrusion of aplitic and pegmatitic dikes

ary Himalayan structures and their related metamorphism (Tab. 1), the metamorphic zones of the early metamorphism of Barrovian type related to the Shikar Beh Nappe stack, thirdly, the retrograde metamorphism associated with the Crystalline Nappe structures will be described and finally the thermo-barometric study of the Crystalline Nappe retrograde metamorphism. A last chapter presents a synthesis and the conclusions.

## Early NE-verging movements: Tandi Syncline, Shikar Beh Nappe and regional Barrovian metamorphism

The geological profile (Fig. 1) and the map of metamorphic zones (Fig. 3) show that the amplitude of the Shikar Beh nappe estimated between the hinge of the Tandi syncline and the position of the frontal part located in the Baralacha La region is approximately 50 km. The frontal part of this nappe has been eroded, but the structures of its internal part can be studied within the High Himalayan Crystalline exposed in the Kulu Valley transect.

Two phases of NE verging folding ( $F_{1a}$ ,  $S_{1a}$  and  $F_{1b}$ ,  $S_{1b}$ ) are restricted to the amphibolite facies grade metamorphic rocks of the Kulu and the Chandra Valleys between Kulu and Khoksar (Figs 2, 4 and 5). In pelitic rocks the existence of the first schistosity ( $S_{1a}$ ) is often revealed by quartz-veins (Figs 5 and 7). The mineral paragenesis of the biotite, garnet, kyanite and staurolite zones associated with the quartz veins represents the highest temperature recorded by the regional metamorphism. The end of crystallisation of the high temperature mineral assemblages post-dates

the second  $S_{1b}$ -schistosity as suggested by the crystallization of non oriented staurolite and kyanite blasts in the metapelites from Khoksar and of biotite poikiloblasts in the low grade metamorphic rocks of the biotite zone. A very strong, NE-oriented, stretching-lineation characterises the two schistosities. Sheath-folds are common along the Rohtang Pass road, between Koti and Marhi. Hand specimen scale structures indicate thrusting by simple shear to the NE. At a higher tectonic level of the Shikar Beh Nappe, in the Tandi Synclines, the first  $S_{1a}$ -schistosity represents the main deformational structure (Fig. 6).

## Main SW-verging deformations: Crystalline Nappe, Main Central Thrust and synkinematic retrograde metamorphism

In the Kulu Valley, the NE-verging structures of the Shikar Beh Nappe are overprinted by SWverging Folds ( $F_2$ ,  $S_2$  and  $F_{2a}$ ,  $AS_{2a}$ , Figs 2, 4, 5, 7, 8 and 9) of the Crystalline Nappe. A strong NEoriented stretching lineation and hand specimen to outcrop scale shear criteria show that the Crystalline Nappe has been thrust towards the SW (Fig. 10). Predominantly, the strong stretching lineation observed throughout the region corresponds probably to an early L1 lineation related to the Shikar Beh Nappe transposed and stretched again by the younger L2 lineation related to the Crystalline Nappe. At a larger scale, the stretching lineation parallel to the transport direction has a remarkably constant orientation perpendicular to the main strike direction of the Himalayan chain (MATTAUER, 1975; BRUNEL, 1986; Jain and Anand, 1988; Mattauer and

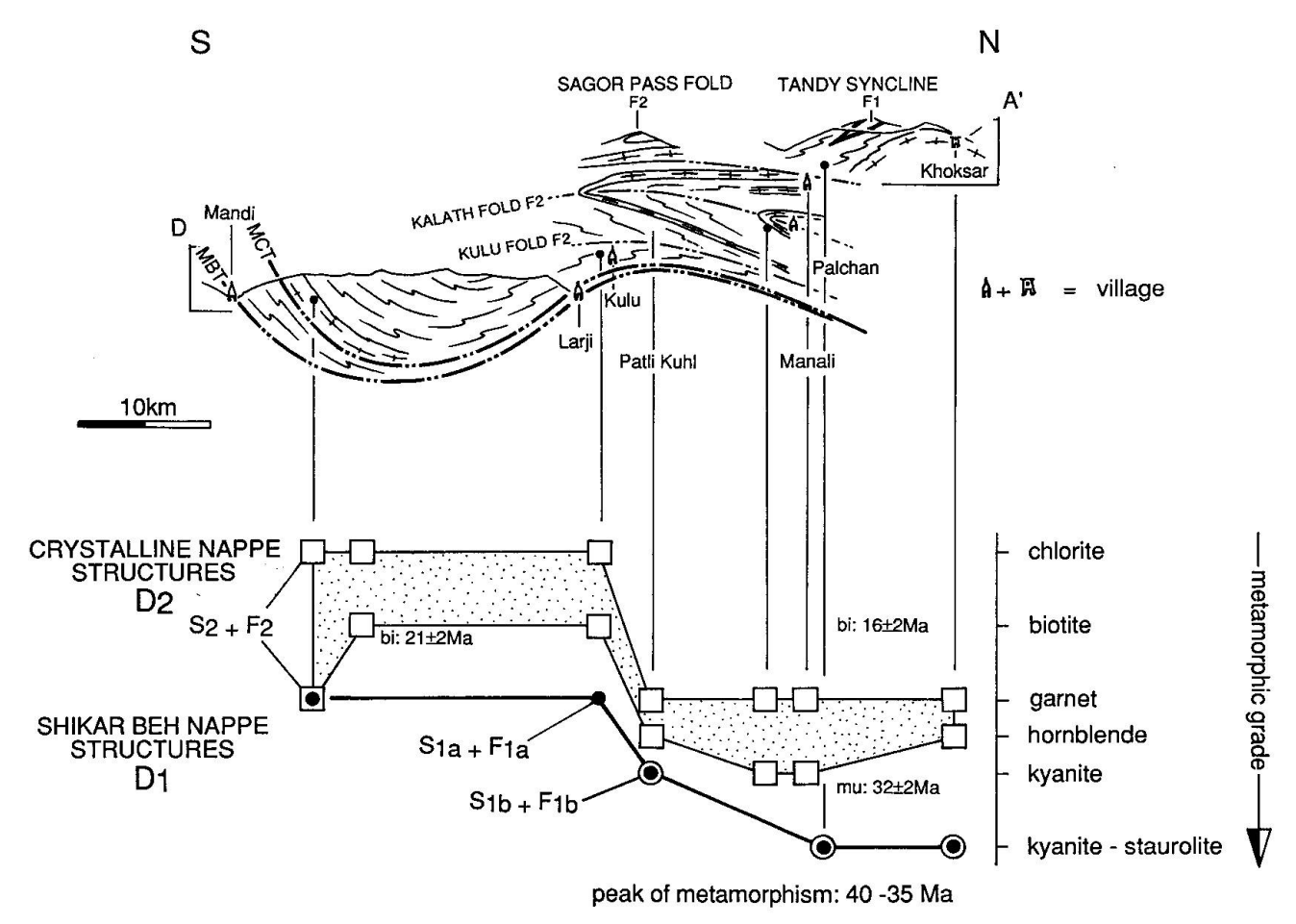


Fig. 4 Crystallization and deformation history of the Shikar Beh Nappe and the Crystalline Nappe. mu = muscovite (500 °C) and bi = biotite (300 °C) Rb-Sr cooling ages after Frank et al. (1977a).

Brunel, 1989; Stäubli, 1989; Guntli, 1993). Deformation occurred under retrograde metamorphic conditions, but still at an amphibolite facies grade (kyanite zone) in a deep tectonic level between Khoksar and Kulu and under greenschist facies conditions (biotite zone) in a higher tectonic level (Tandy Syncline area) and in the frontal part of the nappe between Kulu and Mandi (Fig. 4).

Between Kulu and Manali, a spectacular SW vergent  $F_{2a}$ -fold, the Kalath fold, has been formed during the thrusting of the Crystalline Nappe on the Main Central Thrust towards the SW (Figs 2, 10 and 11; Thöni, 1977, geological map and Fig. 14). An interesting relationship between folding and schistosity can be observed. The  $AS_{2a}$ -axial surface of this SW-verging  $F_{2a}$ -fold is obliquely cut by the steeper and equally SW-verging  $S_{2b}$ -schistosity, probably formed in the late stages of the progressive and rotational deformation (Figs 2, 12). The large-scale fold structures of the Crystalline Nappe have a SW-vergence and indicate a thrusting of the nappe to the SW (Kalath Anticline and Kulu Syncline on Figs 2 and 10). During

the Crystalline Nappe phase of the Tertiary Himalayan Orogeny the metamorphic rocks of the Shikar Beh Nappe were thrust towards the

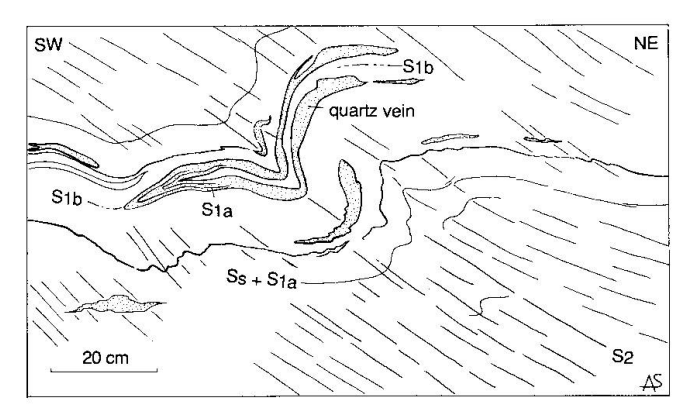


Fig. 5 Tertiary structures in the metapelites of Khoksar: The two  $S_{1a}$ - and  $S_{1b}$ -schistosities are related to the amphibolite facies metamorphism of the Shikar Beh Nappe, with syn- and post-kinematic crystallization of kyanite and staurolite. The third  $S_2$ -crenulation cleavage, created under retrograde metamorphic conditions, is related to the SW-verging  $F_2$ -folds of the Crystalline Nappe.

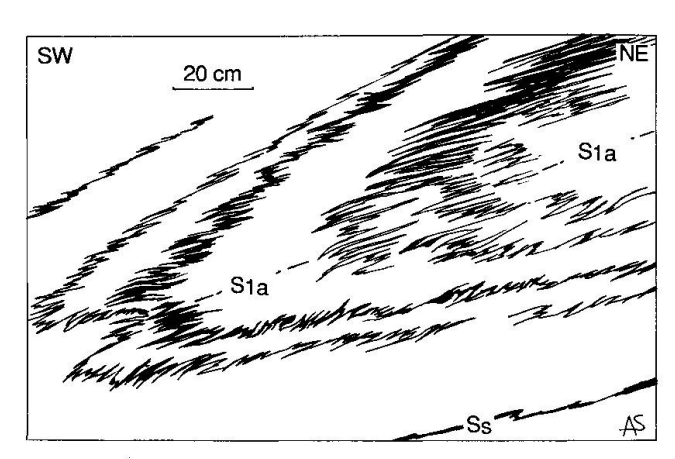


Fig. 6 Stratification Ss,  $F_{1a}$ -fold and  $S_{1a}$ -schistosity in the marbles of the Tandi Syncline (Seki Nala, N of Dhundi, Solang Valley).

SW onto the very low grade metamorphic rocks of the Larji-Kulu-Rampur Window and onto the unmetamorphosed Ganges Molasse at Mandi (Frank et al. 1973, 1977b; Thöni, 1977; Grasemann, 1993). The thrust amplitude of the Crystalline Nappe is greater than 100 km (Fig. 3).

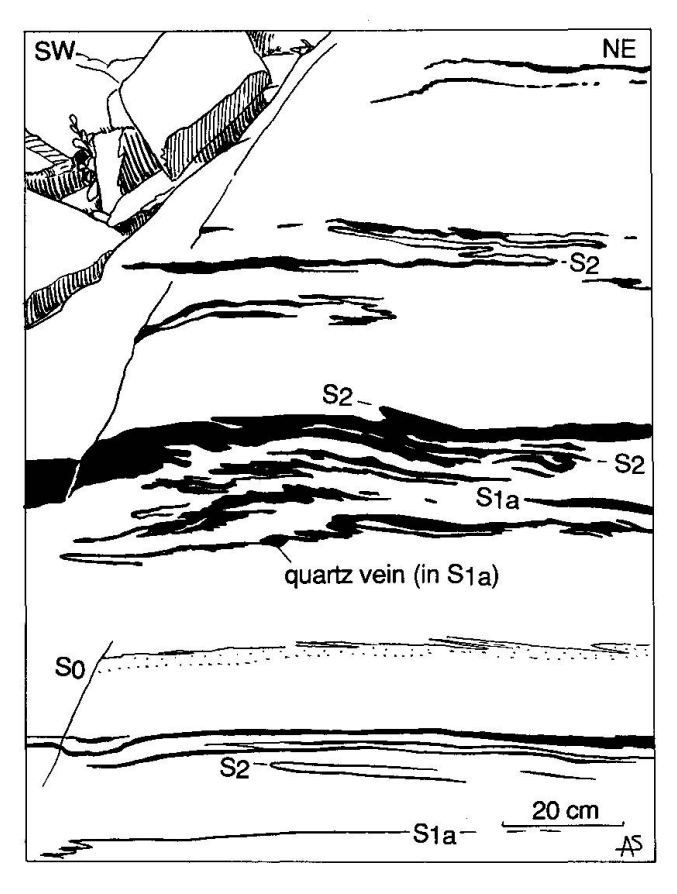


Fig. 7 The first  $S_{1a}$ -schistosity with quartz veins, attributed to the Shikar Beh Nappe, is overprinted by SW-verging  $F_2$ -folds and the main  $S_2$ -schistosity of the Crystalline Nappe and the Main Central Thrust (bridge at the entrance of the Mahui Kad, 5 km south of Kulu).

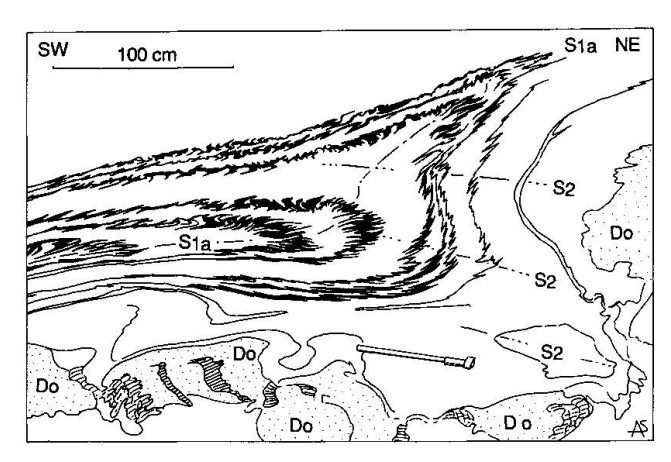


Fig. 8 SW-verging  $F_2$ -folds of the Crystalline nappe overprinting a NE-verging  $F_{1a}$ -anticline in the Tandi marbles, Seki Nala north of Dhundi (Do = boudins of dolomitic marble).

Apart from the Main Central Thrust, we were not able to distinguish any other important thrust structures. The stratigraphic sequence is folded throughout the study area, and generally not disturbed by thrust planes. The hypothetical Halindi Thrust is an exception (Fig. 2). Its existence is revealed by the superposition of different metamorphic mineral assemblages (Figs 14 and 16). In the upper Halindi Nala north of Manali, staurolite-kyanite and garnet bearing two mica schists are overlying kyanite-garnet-biotite-metapelites. The superposition of metapelites of higher metamorphic grade on metapelites of lower grade

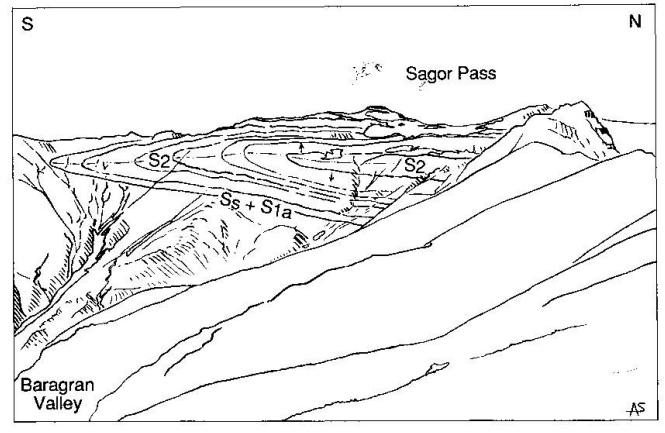
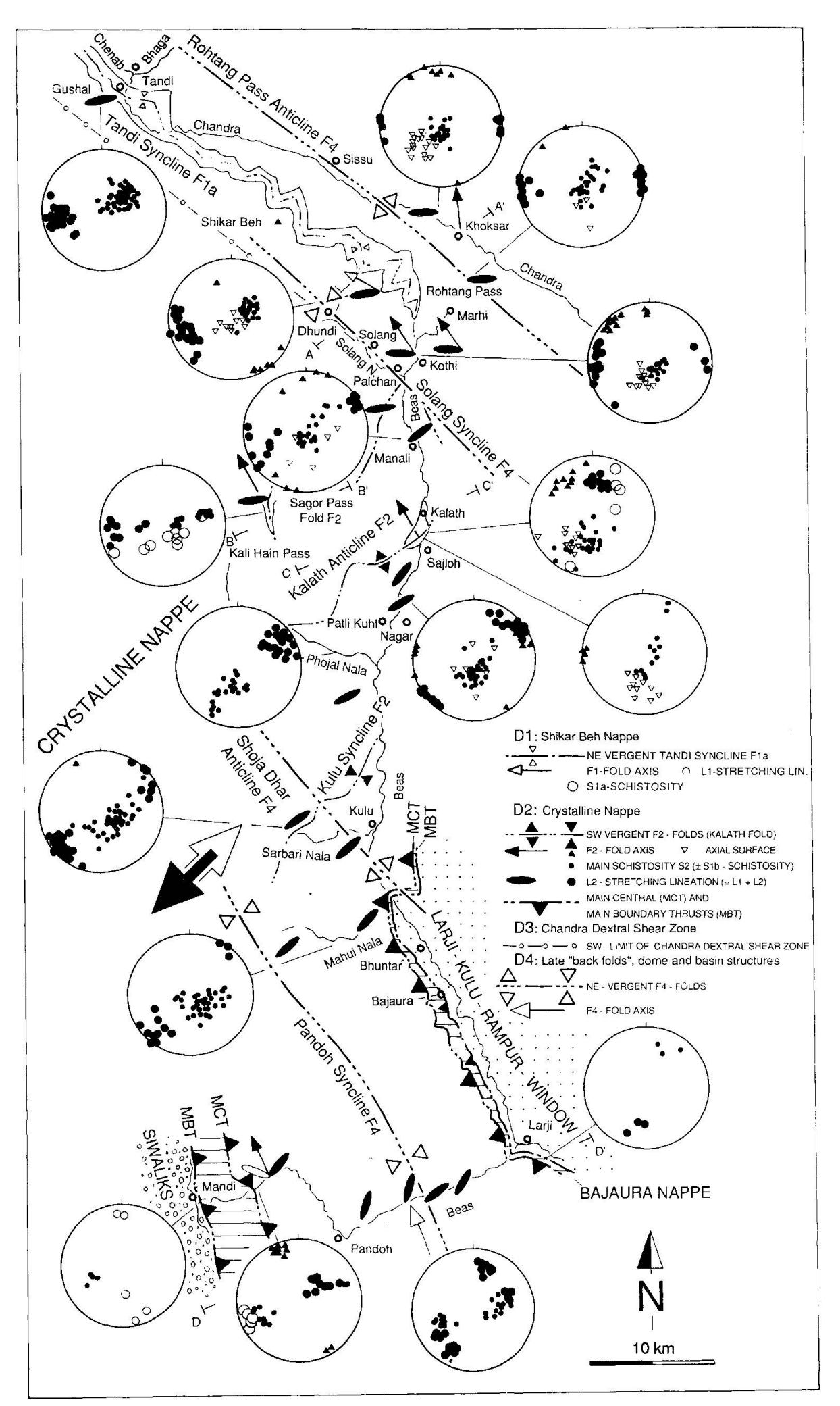


Fig. 9 The SW-verging Sagor Pass Fold belongs to the  $F_2$ -fold generation of the Crystalline Nappe ( $F_2$ -fold axis: 330°/15°). Ss: stratification;  $S_{1a}$ : first schistosity of the Shikar Beh Nappe, arrows indicate stratigraphic younging.

Fig. 10 Structural map of the Crystalline Nappe along the Kulu Valley (Beas River) transect (Lambert equalarea projection, lower hemisphere).



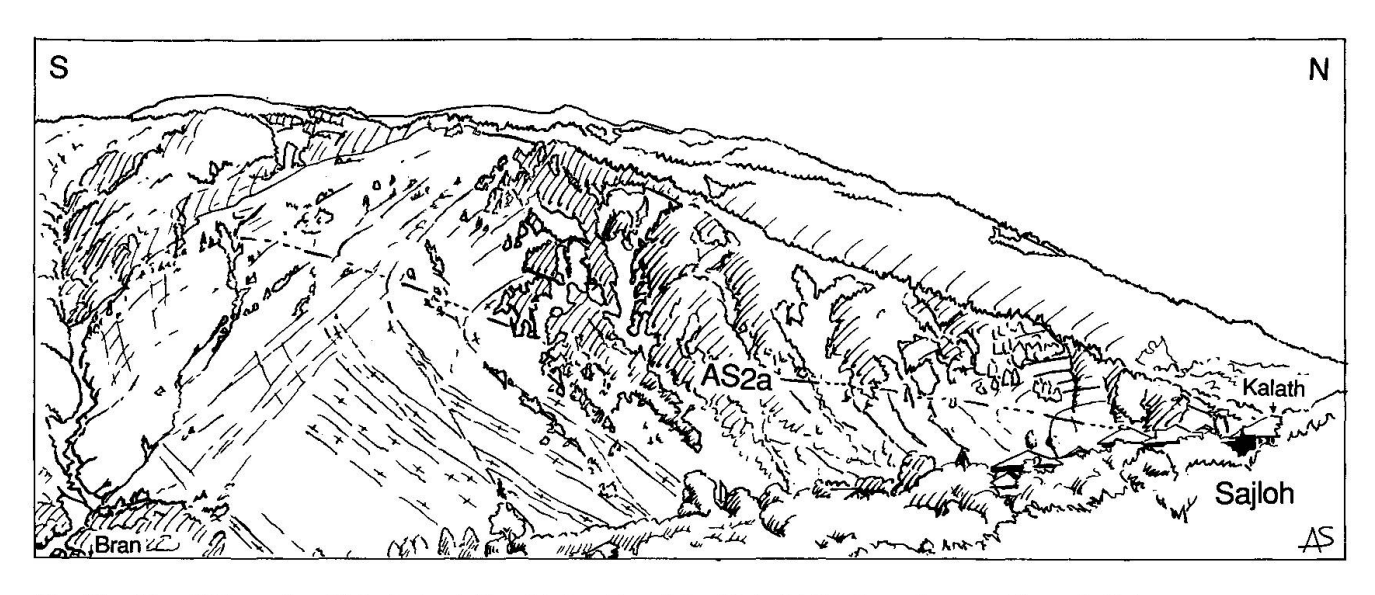


Fig. 11 The SW-verging Kalath Anticline (right side of the Kulu Valley) as observed from Sajloh.

may be due to a thrust. The kyanites and staurolites above the hypothetical stratiform Halindi thrust are deeply altered and partly replaced by white mica. The replacement of staurolite and kyanite by muscovite may be related to the retrograde recrystallization during the late SW-oriented thrusting of this tectonic element within the Crystalline Nappe.

## **Dextral transpression and backfolding**

A map scale dextral shear zone, the Chandra Dextral Shear Zone, is responsible for the late E-W reorientation of the linear structures in the Chandra Valley-Rohtang La region (Fig. 10 and

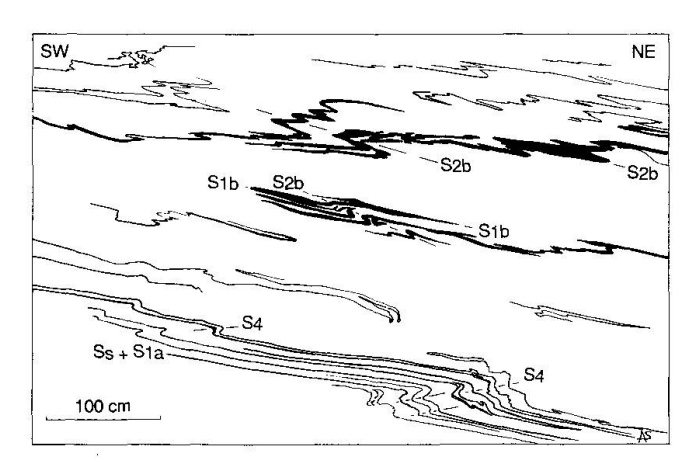


Fig. 12  $S_{1a}$ -quartz veins, schistosity and NE-verging  $F_{1b}$ -folds are overprinted by the SW-verging  $F_{2b}$ -folds and associated  $S_{2b}$ -crenulation cleavage and late NE-verging  $F_4$ -folds (gorge about 500 m above the village of Bran in the overturned and frontal limb of the Kalath  $F_2$ -anticline).

VANNAY, 1993; VANNAY and STECK, in press). The relative ages of the late dextral shear, the NEverging F4-backfolding, the late extension and the intrusion of pegmatitic and aplitic dikes cannot be well constrained by the field observations. Different successions of structures have been observed in the Mandi-Hemis transect of the NW Himalaya (Fig. 1). For instance, in the Nyimaling region, dextral shear occurred before, during and after the formation of the NE-verging Nyimaling dome. In the Sarchu region, the NE-verging backfolds are cut by two generations of normal faults. It is possible that all these structures are various expressions of map scale dextral shear zones, characterized by dome and pull-apart basin structures, normal faults related to transtension and NE-verging folds related to transpression. In the study area, the dextral shear zone of the Chandra Valley and the late extension structures (described below) are perhaps various expressions of a dextral transfension zone. Similar late kinematic dextral shear zones, which are responsible for the E-W transposition of older stretching lineations, are described in other regions of the Himalayan chain (Burg et al., 1984; GAPAIS et al., 1984, 1992; Brun et al., 1985; NI and BARAZANGI, 1985; PÊCHER and BOUCHEZ, 1987; Pêcher, 1989, 1991; Pêcher and Scaillet, 1989; MATTAUER and BRUNEL, 1989; ENGLAND and MOL-NAR, 1990; Pêcher et al., 1991).

#### NE-verging F<sub>4</sub>-"backfolds"

NE vergent F<sub>4</sub>-backfolds are observed all along the transect between Mandi and Khoksar. The main structures are the Pandoh F4-syncline, be-

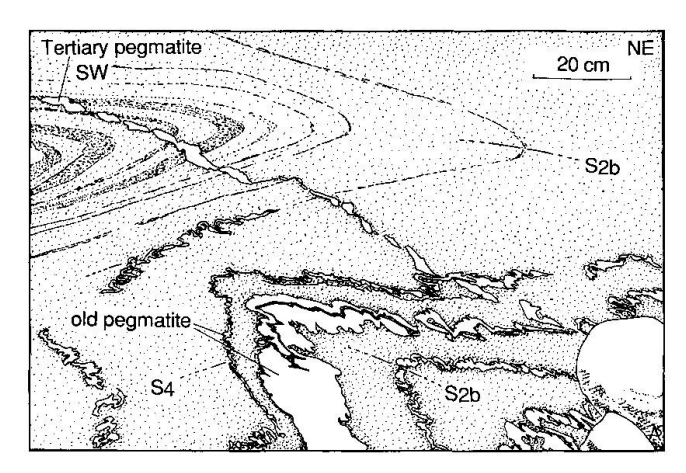


Fig. 13 Late kinematic and post- $F_2$  pegmatitic dike (white) in the hinge zone of the SW-verging Kalath Anticline (gorge 500 m above the Village of Bran). The old pegmatites are probably the same age as the Cambro-Ordovician granitic intrusions (country rock: metagrauwacke of the Phe Formation).

tween Mandi and Larji, the Shoja Dhar F4-anticline forming the Larji-Kulu-Rampur dome, the Solang F4-syncline, north of Manali and the Rohtang Pass F4 anticline or Rohtang pass dome (Figs 2 and 10). It is difficult to know if the map scale dome and basin structures and the outcrop scale backfolds are due to the same or two different phases of deformation. The fold axes have similar NW-SE orientations.

# Late extensional structures: intrusion of aplitic and pegmatitic dikes

Cross-cutting postkinematic pegmatitic dikes are common in the amphibolite facies grade rocks between Patli Kuhl, in the Kulu Valley, and Khoksar in the Chandra Valley (Fig. 13). Near Khoksar the pegmatites are associated with 10 cm to 30 cm thick aplites. These aplites are probably related to the Early Miocene leucogranitic intrusions of the Himalaya, which are located in zones of dextral transtension (Burg et al., 1984; Guillot, 1993; Vannay, 1993; Vannay and Steck, in press).

# Metamorphic zones of the Shikar Beh Nappe and the Crystalline Nappe

164 rock samples have been examined in thin section and the relation between crystallization and deformation established. Paragenesis and relics of an older Barrovian-type metamorphism and younger retrograde mineral assemblages have been identified. The older metamorphism is

related to the Shikar Beh Nappe stack. Its grade ranges from kyanite-staurolite-garnet zone near Khoksar, Palchan and in the upper Halindi Nala to biotite-garnet zone near Larji (Figs 14 and 16a). The regional distribution of staurolite is not so extensive as indicated on Thöni's (1977) map.

The crystallization of the younger retrograde mineral assemblages is related to the deformations that occurred during the cooling of the preexisting Shikar Beh Nappe metamorphism and deformation related to the Crystalline Nappe thrusting. Two metamorphic zones can be distinguished: a greenschist facies zone, with chlorite, biotite and sometimes garnet, between Mandi and Kulu and very low grade amphibolite facies zone, with biotite, garnet, hornblende and kyanite between Patli Kuhl and Khoksar. The regional distribution of index-minerals and their relationship with the deformational structures of the Shikar Beh and Crystalline Nappes is schematically represented on Fig. 4. Figures 15 and 16b show the regional distribution of the indexminerals of the retrograde metamorphism related to the Crystalline Nappe. In the northern Kulu-Khoksar transect, the deformations related to the Crystalline Nappe, as well as those related to the Shikar Beh Nappe, occurred mainly under lower amphibolite facies conditions and for this reason the retrograde metamorphism is not very appar-

#### Geothermometry and geobarometry

To complete the index minerals distribution and crystallization-deformation studies, 21 samples have been selected for temperature and pressure estimations using mineral assemblages of the Crystalline Nappe. Experimental techniques and mineral analyses are given in the appendices.

Twenty garnet-biotite temperatures were used to determine the temperature distribution within the Crystalline Nappe. Three calibrations were tested: Ferry and Spear (1978), Hodges and Spear (1982) and Ganguly and Saxena (1984). The analyzed garnets have a varying and sometimes rather high Ca content. Therefore, a correction was applied to the Ferry and Spear (1978) calibration. Most of our conclusions rely on temperature variations and not on absolute values, the choice of a calibration is therefore not crucial.

The temperature estimates based on the garnet-biotite geothermometer using the Hodges and Spear (1982) calibration are plotted on the schematic geological section of the Crystalline Nappe of the Kulu Valley (Fig. 16c). The temperature distribution yields a coherent picture. It is

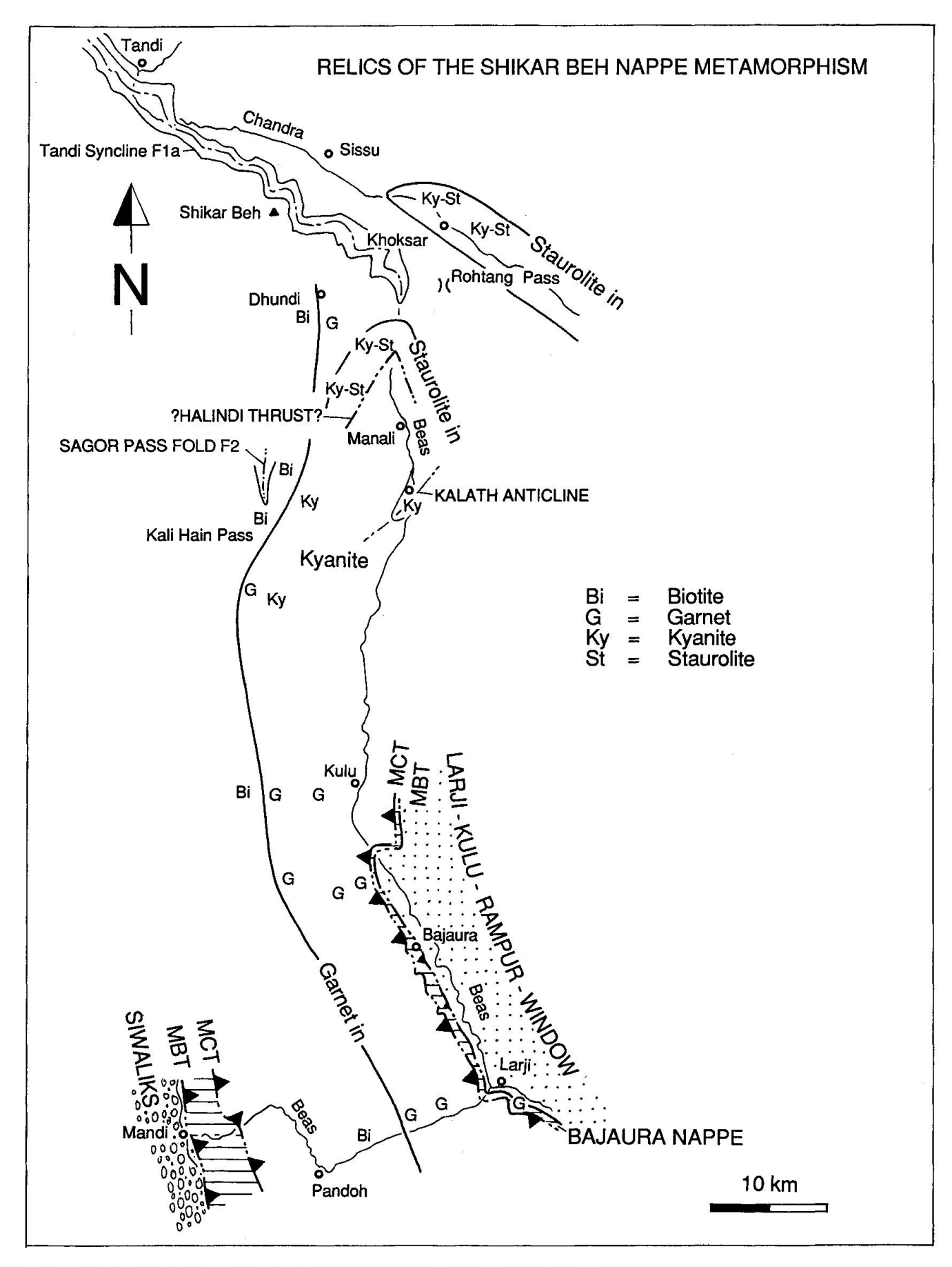


Fig. 14 Relics of the Shikar Beh Nappe metamorphism of the Kulu Valley transect.

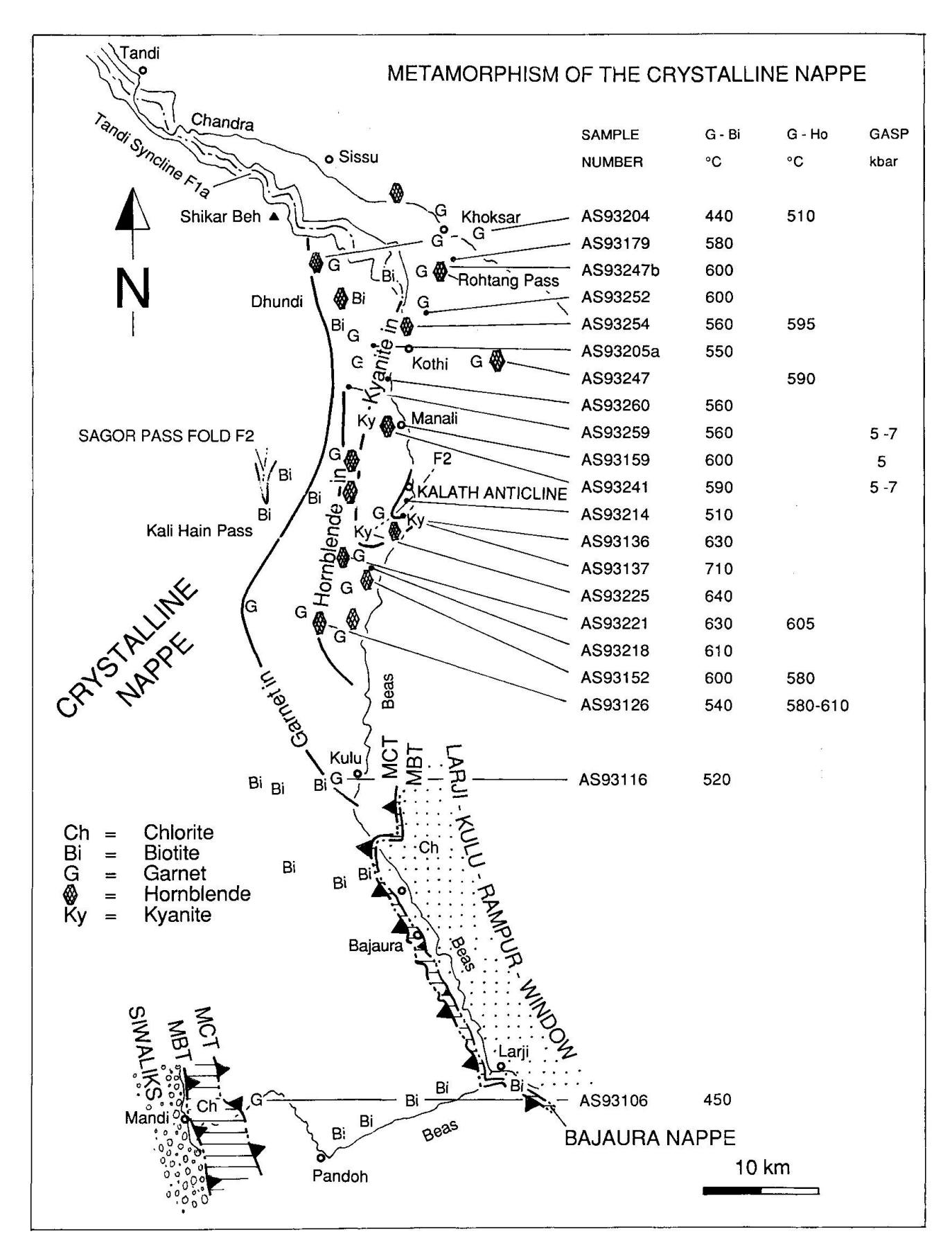
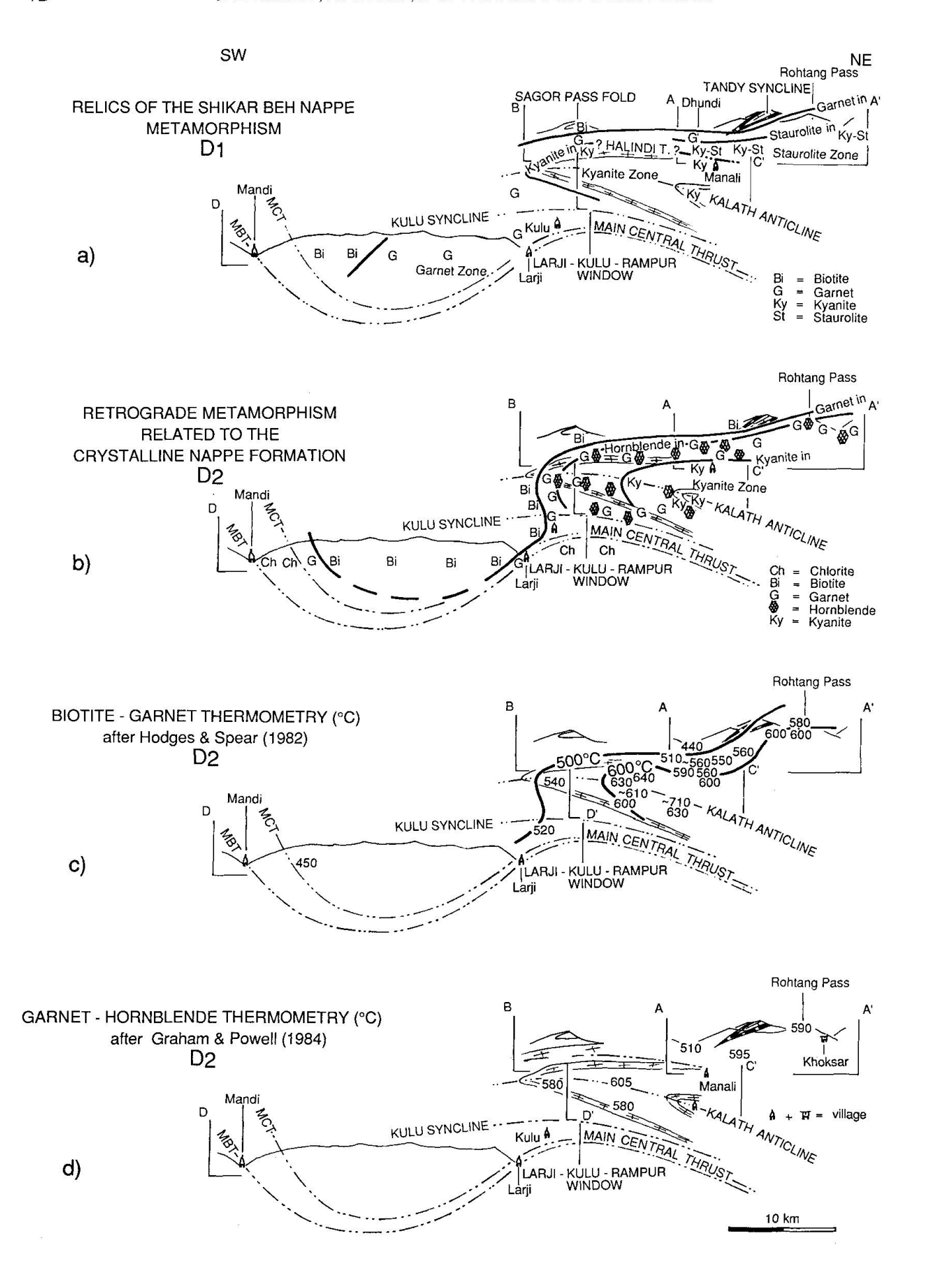


Fig. 15 Metamorphism, garnet-biotite temperatures (calibration Hodges and Spear, 1982), garnet-hornblende temperatures (calibration Graham and Powell, 1984) and GASP geobarometry (calibration Hodges and Spear, 1982) of the Crystalline Nappe of the Kulu Valley transect.



possible to draw the 500 °C and 600 °C isotherms, indicating temperatures increasing from south to north up the Kulu Valley and also a normal vertical temperature gradient between Kulu and the Rohtang Pass. Near Kulu, the 500 and 600 °C isotherms are folded by the Kalath and Kulu folds, but not as much as the older main S<sub>1b</sub>-schistosity in the SW-verging Kalath Anticline, which is cut by the 600 °C isotherm. This geometric relationship suggests that thrusting of the Crystalline Nappe occurred at high temperature and that the temperature distribution has been influenced by heat flow related to cooling by erosion and overthrusting of the hot Crystalline Nappe on the colder rocks of the Larji-Kulu-Rampur Window. The garnet-biotite temperature distribution corroborates the post-temperature peak and synmetamorphic thrusting of the Crystalline Nappe deduced from the crystallization-deformation relationships (Fig. 4). The temperatures obtained from the garnet-biotite thermometry could represent the period between the peak of metamorphism and the late retrograde conditions. Comparing the stable mineral-paragenesis with the temperature obtained from the Hodges and Spear (1982) calibration we observe that the calculated temperature is always about 50 °C higher than the temperature estimated from the hornblende-plagioclase-in isograd (Figs 17 and 18).

To complete the garnet-biotite geothermometry, some garnet-hornblende assemblages were analyzed. Six samples were analyzed, five of which contain also the garnet-biotite assemblage. The results of temperatures from the Graham and Powell (1984) calibration are given in figure 16d.

To better constrain the model and the geothermometry data, some analyses were performed using the garnet-kyanite-quartz-plagioclase (GASP) barometer. Three samples, all lo-

Fig. 16 Metamorphism in the Kulu Valley transect. Cross sections from Mandi to Rohtang Pass and Khok-

cated in the Manali region, contain the GASP assemblage. In figure 19, the intersection area between the P-T lines for the garnet biotite geothermometer and for the GASP geobarometer (both using the calibrations of Hodges and Spear, 1982) are plotted on a pressure temperature diagram. Pressures from 5 to 7 kbar and temperatures around 550 °C can be deduced from this diagram. It corresponds to a thermal gradient of about 22–30 °C/km.

### Synthesis and conclusions

The new field observations (Figs 2 and 10) confirm the excellent geological maps drawn by Frank et al. (1973), Thöni (1977) and Grase-MANN (personal communication). Along the Kulu Valley transect, the structures and metamorphism observed in the metasediments and metagranites of the High Himalayan Crystalline are all related to the Himalayan Orogeny. No evidence of any deformational structures related to an older compressional orogenic belt in the Upper Precambrian to Jurassic sedimentary sequence as proposed by Jain et al. (1980) was found. Relics of a high pressure metamorphism, as observed by Pognante and Lombardo (1989) and Pognante et al. (1990) in the High Himalayan Crystalline of SE Zanskar, have not been observed in the study

The field observations from summer of 1993 and new laboratory data corroborate the model proposed by STECK et al. (1993 a and b), VANNAY (1993) and Vannay and Steck (in press) for the tectonic evolution of the High Himalayan Crystalline. The High Himalayan Crystalline has suffered a complex tectono-metamorphic history with two major phases of nappe emplacement (Fig. 20). Crustal thickening of the High Himalayan Crystalline started in the Shikar Beh (Rohtang La) region with the formation of the NEverging and intracontinental Shikar Beh Nappe stack perhaps due to the reactivation of a SWdipping intracontinental listric normal fault of the North-Indian flexural passive margin (VANNAY, 1993).

According to geochronologic data from Frank et al. (1977b), Le Fort (1986, 1989), Mehta (1977 and 1978), Pande and Kumar (1974) and Treloar and Rex (1990), the temperature peak of the Himalayan Barrovian metamorphism was reached some 40 to 35 Ma ago, before the 32 ± 2 Ma Rb-Sr-muscovite cooling age obtained by Frank et al. (1977a). The arrival in the Baralacha La region of the frontal part of the SW-directed Nyimaling-Tsarap Nappe is a little

a) Distribution of relics of index-minerals related to the Shikar Beh Nappe metamorphism.

b) Distribution of index-minerals related to the retrograde metamorphism of the Crystalline Nappe.

c) Temperature estimates of the retrograde metamorphism of the Crystalline Nappe using the biotite-garnet geothermometer (calibration HODGES and SPEAR, 1982), P = 5 kbar.

d) Temperature estimates of the retrograde metamorphism of the Crystalline Nappe using the garnet-horn-blende geothermometer (calibration Graham and Powell, 1984), P = 5 kbar.

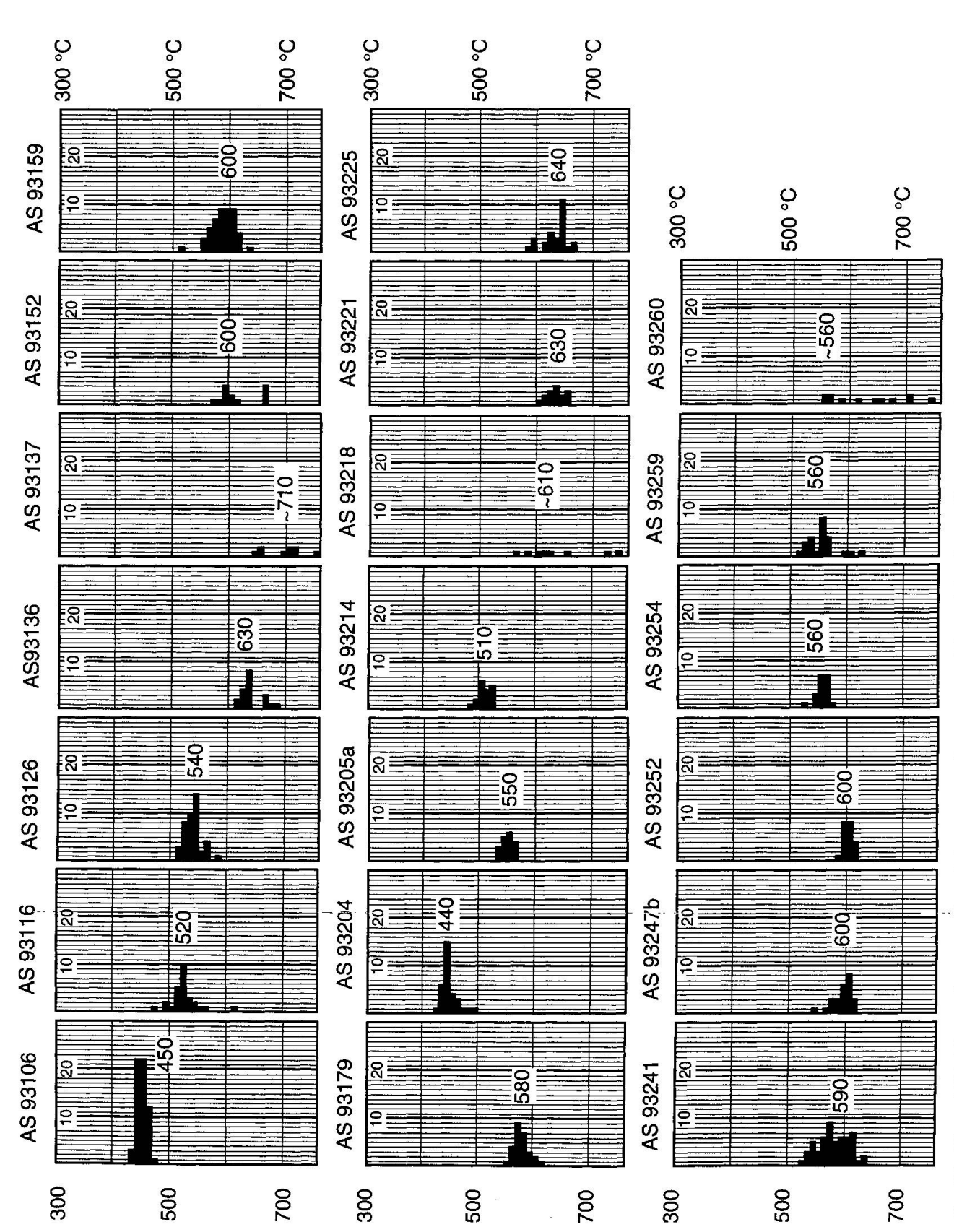


Fig. 17 Garnet-Biotite geothermometry of the retrograde metamorphism of the Crystalline Nappe (calibration Honges and Spear, 1982), P = 5 kbar.

younger than the formation of the NE-verging Shikar Beh Nappe stack.

The formation of the SW-vergent folds of the Crystalline Nappe and the Main Central Thrust is younger and was postpeak metamorphic but still at high temperatures. The Crystalline Nappe has been thrust towards the SW before cooling down to 300 °C,  $21 \pm 2$  Ma ago (Rb-Sr-biotite-cooling age, Frank et al., 1977a). The onset of this thrusting is probably older than the intrusion of the leucogranites 24-22 Ma ago (U-Pbmonazite age on the Oji Bihal granite François Bussy, personal communication; Ar-Ar age on the Gunjerab granite, VILLA and ODDONE, 1988). Thrusting, rapid isostatic uplift and erosion are responsible for the cooling of the High Himalayan Crystalline. The amplitude of the displacement towards the SW of the Crystalline nappe along the Main Central Thrust is in excess of 100 km. The

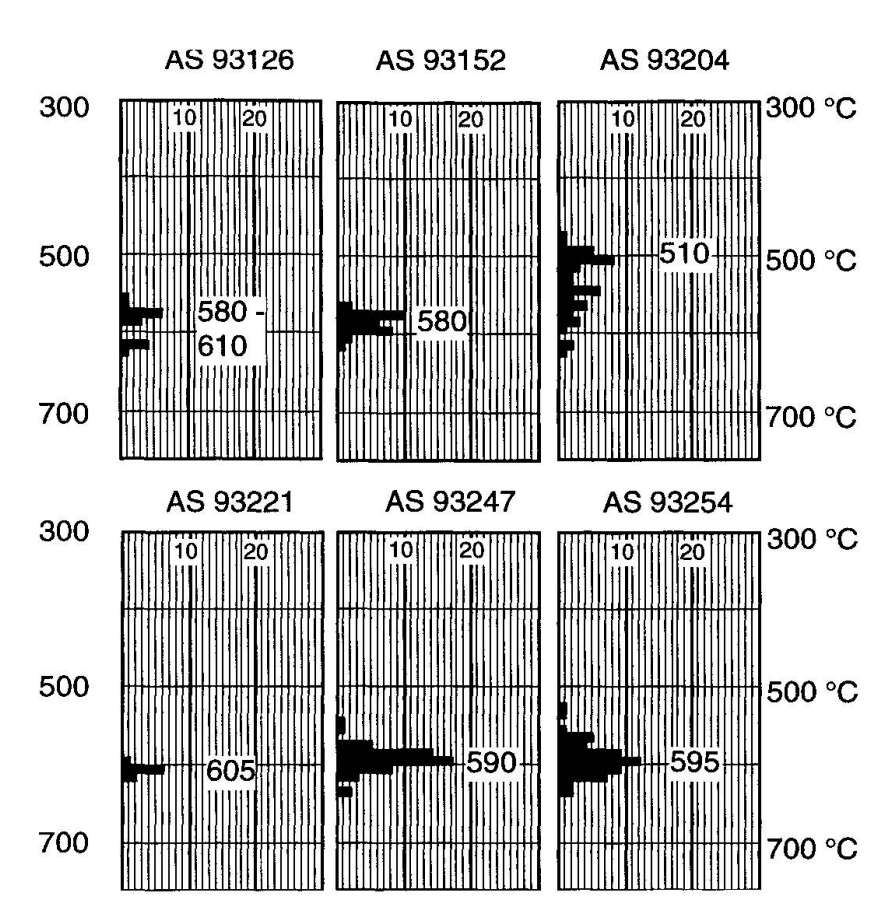


Fig. 18 Garnet-Hornblende geothermometry of the retrograde metamorphism of the Crystalline Nappe (calibration Graham and Powell, 1984), P = 5 kbar.

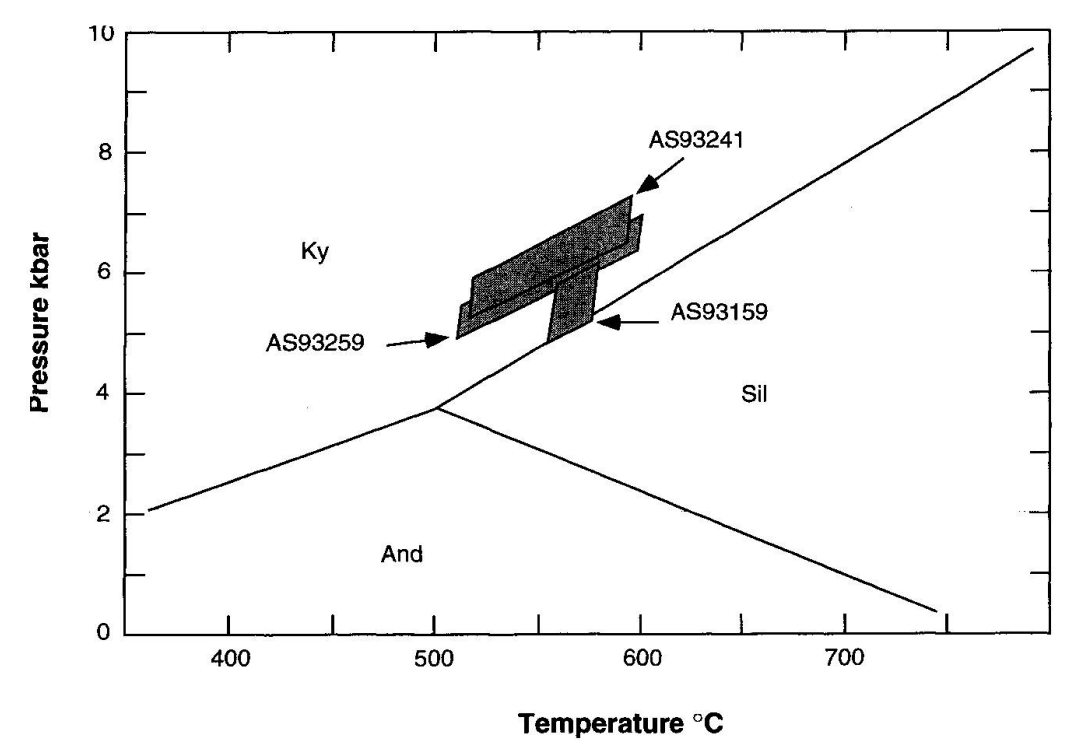
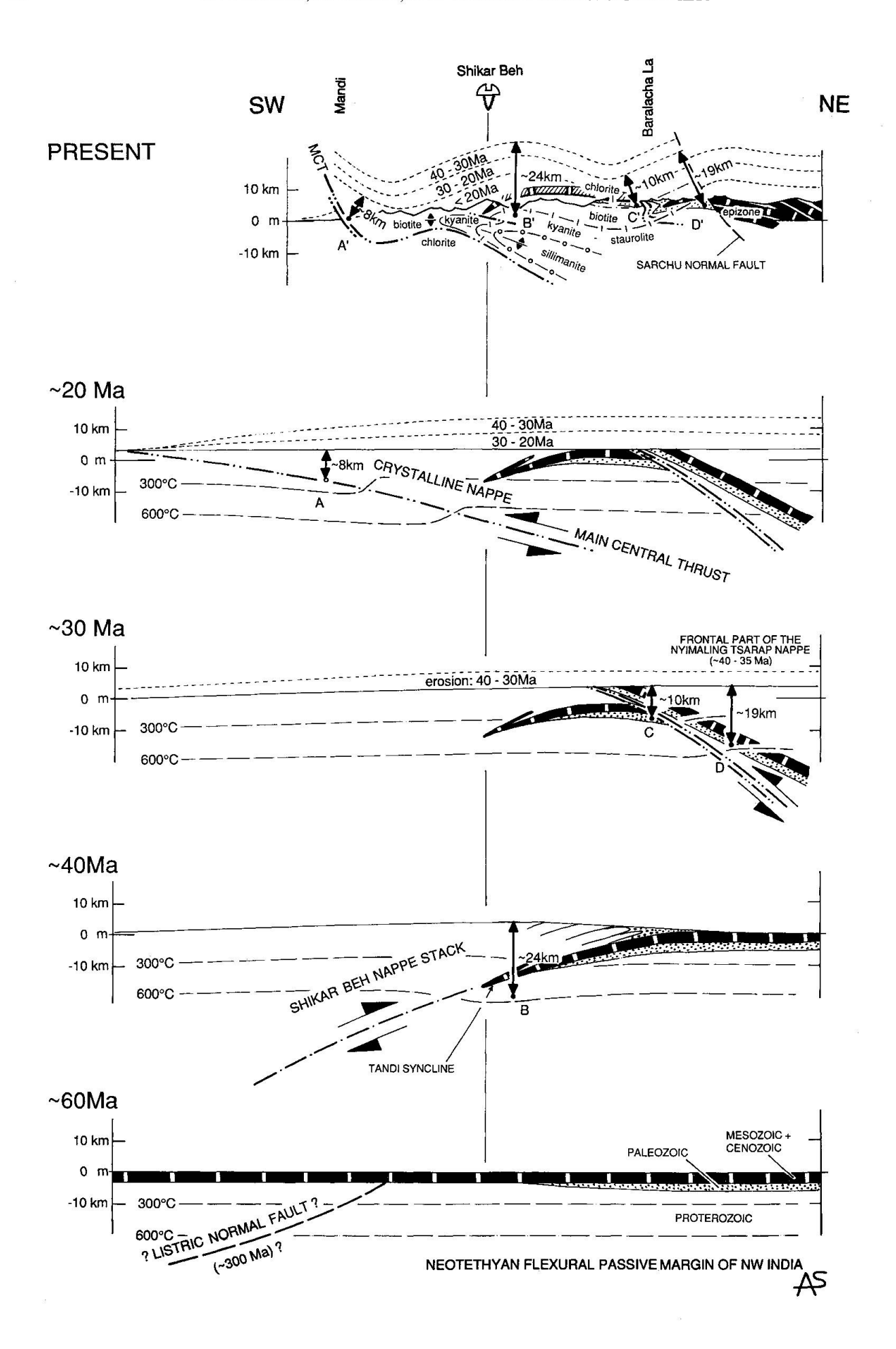


Fig. 19 Pressure and temperature estimation of three qz-mu-bi-pl-gr-ky schists of the retrograde Crystalline Nappe metamorphism, using the garnet-biotite geothermometer and the GASP geobarometer (both calibrations HODGES and Spear, 1982). Sample location on figure 15; Al<sub>2</sub>SiO<sub>5</sub> triple point from Holdaway (1971).



formation of the Crystalline Nappe is followed by dextral shear and the creation of great dome and basin structures as well as NE-verging backfolds. The Chandra Dextral Shear Zone located in the Rohtang Pass and Chandra Valley region is responsible for the E-W transposition of the preexisting NE-SW oriented stretching-lineations (VANNAY, 1993; VANNAY and STECK, in press). Aplitic veins are situated in this dextral shear zone, suggesting that intracrustal dextral shear is followed by, or accompanies transfension and extension. In the Zanskar region, the late leucogranite intrusions have an age of 24-22 Ma (Oji Bihal granite, monazite U-Pb ages, François Bussy, personal communication).

#### Acknowledgements

Financial support from the Herbette Foundation (Lausanne University) for the summer 1993 field work is gratefully acknowledged. We thank François Bussy for discussion and help with the microprobe analyses. We are indebted to Jean-Pierre Burg and Dan Marshall who reviewed the manuscript and to Wolfgang Frank, Bernhard Grasemann, Peter Guntli and Martin Thöni for fruitful discussions.

Jean-Luc Epard, Albrecht Steck and Jean-Claude Vannay acknowledge support from the Swiss National Science Foundation (20-37470.93 and 20-38917.93).

Fig. 20 Kinematic model for the Cenozoic tectonometamorphic evolution of the High-Himalaya in the Kulu Valley-Lahul-SE Zanskar area (NW Himalaya). The initial situation represents a part of the NW Indian margin of the Neotethys as reconstructed by STECK et al. (1993 a and b) and VANNAY (1993). Maximal thickness for the Mesozoic-Cenozoic sequence has been extrapolated to the entire section. The Shikar Beh Nappe could be the consequence of an older intracrustal extensional fault related to the Neotethyan rifting (STECK et al., 1993 a and b, Vannay and Steck, in press). As the structures of the frontal part of the Nyimaling-Tsarap Nappe are superposed to those related to the Shikar Beh Nappe, the initiation of the former unit to the north is most probably coeval or even older than the development of the latter unit. The Shikar Beh Nappe stack and the Nyimaling-Tsarap Nappe are responsible for early Paleogene regional metamorphism with peak temperatures prior to 32 Ma for the Shikar Beh Nappe metamorphism (Rb-Sr white mica cooling age, FRANK et al., 1977a) and before 33.5 Ma for the Nyimaling-Tsarap Nappe metamorphism (40Ar/39Ar cooling age for amphibole, total gas age, Spring et al. 1993a). The development of the Crystalline Nappe occurred in Neogene time with crystallization and deformation during cooling and erosion (Rb-Sr biotite cooling ages of 21 and 16 Ma for biotite, Frank et al., 1977a). Based on our P-T estimations, an average uplift and erosion rate of 0.6 mm/y has been chosen for this model.

#### References

Baud, A., Arn, R., Bugnon, P., Crisinel, A., Dolivo, E., Escher, A., Hammerschlag, J.G., Marthaler, M., Masson, H., A., S. and Tièche, J.C. (1982): Le contact Gondwana/péri-Gondwana dans le Zanskar oriental (Ladakh, Himalaya). Bull. Soc. géol. France 24(2), 341–361.

BAUD, A., GAETANI, M., GARZANTI, E., FOIS, E., NICORA, A. and TINTORI, A. (1984): Geological observations in southeastern Zanskar and adjacent Lahul area (northwestern Himalaya). Eclogae geol. Helv.

77(1), 171–197. Brun, J.P., Burg, J.P. and Cheng, G.M. (1985): Strain trajectories above the Main Central Thrust (Himalaya) in southern Tibet. Nature 313, 388–390.

Brunel, M. (1986): Ductile thrusting in the Himalayas: shear sense criteria and stretching lineations. Tectonics 5(2), 247–265.

BURG, J.P., BRUNEL, M., GAPAIS, D., CHENG, G.M. and Liu, G.H. (1984): Deformation of leucogranites of the crystalline Main Central Sheet in southern Tibet

(China). J. struct. Geol. 6(5), 535–542. ENGLAND, P. and MOLNAR, P. (1990): Right-lateral shear and rotation as the explanation for stike-slip fault-

ing in eastern Tibet. Nature 344, 140-142.

FERRY, J.M. and SPEAR, F.S. (1978): Experimental calibration of the partitioning of Fe and Mg between biotite and garnet. Contrib. Mineral. Petrol. 66,

Frank, W., Hoinkes, G., Miller, C., Purtscheller, F., Richter, W. and Thöni, M. (1973): Relations between metamorphism and orogeny in a typical section of the Indian Himalayas. Tscherm. Mineral. Petrogr. Mitt. 20, 303–332. Frank, W., Thöni, M. and Purtscheller, F. (1977a):

Geology and petrography of Kulu-South Lahul area. Colloq. int. CNRS (Paris) 268, 147-160.

Frank, W., Gansser, A. and Trommsdorff, V. (1977b): Geological observations in the Ladakh area (Himalayas), a preliminary report. Schweiz. Mineral.

Petrogr. Mitt. 57, 89–113. Frank, W., Baud, A., Honegger, K. and Trommsdorff, V. (1987): Comparative studies on profiles across the northwest Himalayas. In: Schaer, J.P. and RODGERS, J. (Eds): The anatomy of mountain ranges (pp. 261-275). Princeton University Press, Princeton.

Frank, W., Grasemann, B., Chonawetz, E. and Miller, C. (1992): Age and palaeographic setting of Proterozoic rock series in the NW-Himalayas. 7th Himalaya-Karakoram-Tibet Workshop, Oxford.

Abstract vol. (p. 26). Fuchs, G. (1982): The geology of Western Zanskar. Jb. geol. Bundesanst. (Wien) 125(1-2), 1-50.

FUCHS, G. (1987): The geology of Southern Zanskar (Ladakh)-Evidence for the autochthony of the Tethys Zone of the Himalaya. Jb. geol. Bundesanst.

(Wien) 130(4), 465–491.

Fuchs, G. (1992): Pre-Alpine and Alpine orogenic phases in the Himalaya. In: Sinha, A.K. (Ed.): Himalayan orogen and global Tectonics (pp. 19–34).

Balkema, Rotterdam.

GAETANI, M., CASNEDI, R., FOIS, E., GARZANTI, E., JADOUL, F., NICORA, A. and TINTORI, A. (1986): Stratigraphy of the Tethys Himalaya in Zanskar, Ladakh: initial report. Riv. Ital. Paleont. Stratigr. 91(4), 443–478.

GAETANI, M. and GARZANTI, E. (1991): Multicyclic history of the northern India continental margin (Northwestern Himalaya). Bull. Amer. Assoc. Petroleum Geol. 75(9), 1427–1446.

GANGULY, J. and SAXENA, S.K. (1984): Mixing properties of aluminosilicate garnets: constraints from natural and experimental data, and applications to geothermo-barometry. American Mineralogist, 69, 88–97.

Gansser, A. (1964): Geology of the Himalayas. Interscience Publishers, London New York Sidney.

- GANSSER, A. (1981): The geodynamic history of the Himalaya. In: GUPTA, H.K. and DELANY, F.M. (Eds): Zagros-Hindu Kush-Himalaya Geodynamic evolution (pp. 111–121). Geodynamic Series 3, Washington.
- Gapais, D., Gilbert, E. and Pêcher, A. (1984): Structures et trajectoires de déformation dans la zone de suture de l'Indus-Tsangpo en Himalaya du Ladakh, région de la Suru. C. R. Acad. Sci. Paris 299(4), 179–182.
- Gapais, D., Pecher, A., Gilbert, E. and Ballèvre, M. (1992): Syn-convergence spreading of the central sheet, Ladakh Himalaya. Tectonics, 11/5, 1054–1056.
- Graham and Powell (1984): A garnet-hornblende geothermometer: calibration testing and application to the Pelona Schists, Southern California. J. met. Geol. 2, 13–31.
- Grasemann, B. (1993): Numerical modelling of the thermal history of the NW Himalayas, Kullu Valley, India. In: Treloar, P.J. and Searle, M.P. (Eds): Himalayan tectonics. Geological Society Special Publication (London), 74, 475–484.
- Guillot, S. (1993): Le granite du Manaslu (Népal Central) marqueur de la subduction et de l'extension intracontinentales himalayennes. Géol. Alpine, Mém. H.S. 19.
- Guntli, P. (1993): Geologie und Tektonik des Higher und Lesser Himalaya im Gebiet von Kishtwar, SE Kashmir (NW Indien). Thèse de doctorat, ETH Zürich.
- Hodges, K.V. and Spear, F. S. (1982): Geothermometry, geobarometry and the Al₂SiO₅ triple point at Mt. Moosilauke, New Hamphshire. American Mineralogist, 67, 1118–1134.
- HOLDAWAY, M.J. (1971): Stability of andalusite and the aluminium silicate phase diagram. Am. J. Sci., 271, 97–131
- Honegger (1983): Strukturen und Metamorphose im Zanskar-Kristallin (Ladakh-Kashmir, Indien). Thèse de doctorat, ETH Zürich.
- Honegger, K., Dietrich, V., Frank, W., Gansser, A., Thöni, M. and Trommsdorff, V. (1982): Magmatism and metamorphism in the Ladakh Himalayas (the Indus-Tsangpo suture zone). Earth and Planet. Sci. Lett. 60, 253–292.
- JAIN, A.K., GOEL, R.K. and NAIR, N.G.K. (1980): Implications of pre-Mesozoic orogeny in the geological evolution of the Himalaya and Indo-Gangetic Plains. Tectonophysics 62, 67–86.
- Jain, A.K. and Anand, A. (1988): Deformation and strain patterns of an intracontinental collision ductile shear zone an example from the Higher Garhwal Himalaya. J. struct. Geol. 10(7), 717–734.
- KÜNDIG, R. (1988): Kristallisation und Deformation im Higher Himalaya, Zanskar (NW-Indien). Thèse de doctorat, ETH Zürich.
- KÜNDIG, R. (1989): Domal structures and high-grade metamorphism in the Higher Himalayan Crystalline, Zanskar region, north-west Himalaya, India. J. metamorphic Geol. 7, 43–55.
- LE FORT, P. (1986): Metamorphism and magmatism

- during the Himalayan collision. In: Coward, M.P. and Ries, A.C. (Eds): Collision tectonics. Geological Society Special Publication (London), 19, 152–172
- LE FORT, P. (1989): The Himalayan orogenic segment. In: Sengor, A.M.C. (Ed.): Tectonic evolution of the Tethyan region (p. 289–386). Kluwer Acad. Publishers, Dordrecht.
- Mattauer, M. (1975): Sur le mécanisme de la formation de la schistosité dans l'Himalaya. Earth and Planet. Sci. Lett. 28, 144–154.
- Mattauer, M. and Brunel, M. (1989): La faille normale Nord-Himalayenne (FNNH) conséquence probable d'un diapirisme granitique. C. R. Acad. Sci. Paris 308, 1285–1289.
- MEHTA, P.K. (1977): Rb–Sr geochronology of the Kulu-Mandi belt: its implications for the Himalayan tectogenesis. Geol. Rdsch. 66, 156–174.
- Mehta, P.K. (1978): Rb-Sr geochronologic of the Kulu-Mandi belt: its implications for the himalayan tectogenesis – a reply. Geol. Rdsch. 68, 383–392.
- NI, J. and BARAZANGI, M. (1985): Active tectonics of the western Himalaya above the underthrusting Indian plate: the upper Sutlej river basin as a pull-apart structure. Tectonophysics 112, 277–295.
- Pande, I.C. and Kumar, S. (1974): Absolute age determinations of crystalline rocks of Manali-Jaspa region, Northwestern Himalaya. Geol. Rdsch. 62(2), 539–548.
- Pêcher, A. (1989): The metamorphism in Central Himalaya. J. metamorphic Geol. 7, 31–41.
- Pècher, A. (1991): The contact between the Higher Himalayan Crystalline and the Tibetan sedimentary series: Miocene large-scale dextral shearing. Tectonics 10(3), 587-598.
- PECHER, A. and BOUCHEZ, J.L. (1987): High temperature decoupling between the Higher Himalaya Crystalline and its sedimentary cover. Terra Cognita 7, 110.
- PÉCHER, A. and SCAILLET, B. (1989): La structure du Haut-Himalaya au Garhwal (Indes). Eclogae geol. Helv. 82(2), 655–668.
- Pecher, A., Bouchez, J.L. and Le Fort, P. (1991): Miocene dextral shearing between Himalaya and Tibet. Geology 19, 683–685.
- POGNANTE, U. and LOMBARDO, B. (1989): Metamorphic evolution of the High Himalayan Crystallines in SE Zanskar, India. J. metamorphic Geol. 7, 9–17.
- Pognante, U., Castelli, D., Benna, P., Genovese, G., Oberli, F., Meier, M. and Tonarini, S. (1990): The crystalline units of the High Himalayas in the Lahul-Zanskar region (northwest India): metamorphic-tectonic history and geochronology of the collided and imbricated Indian plate. Geol. Mag. 127, 101–117.
- Powell, C.M.A. and Conaghan, P.J. (1973): Polyphase deformation in the Phanerozoic rocks of the Central Himalayan Gneiss, Northwest Himalaya. J. Geol. 81, 127–143.
- Powell, C.M.A. and Conaghan, P.J. (1978): Rb-Sr geochronology of the Kulu-Mandi belt: its implications for the himalayan tectogenesis-discussion. Geol. Rdsch. 68, 380-383.
- RICHARDSON, S.W., GILBERT, M.C. and BELL, P.M. (1969): Experimental determination of kyanite-andalusite-sillimanite equilibrium; the aluminium silicate triple point. Amer. J. Sci. 267, 259–272.
- Spring, L. (1993): Structures gondwaniennes et himalayennes dans la zone tibétaine du Haut Lahul-Zanskar oriental (Himalaya indien). Mém. Géol. (Lausanne) 14, 1–148.

- Spring, L. and Crespo-Blanc, A. (1992): Nappe tectonics, extension, and metamorphic evolution in the Indian Tethys Himalaya (Higher Himalaya, SE Zanskar and Upper Lahul). Tectonics 11(5), 978–989.
- Spring, L., Bussy, F., Vannay, J.C., Huon, S. and Cosca, M.A. (1993a): Early Permian granitic magmatism of alkaline affinity in the Indian High Himalaya (Upper Lahul-SE Zanskar): geochemical characterization and geotectonic implications. In: Treloar, P.J. and Searle, M.P. (Eds): Himalayan tectonics. Geological Society Special Publication (London), 74, 251-264.
- Spring, L., Masson, H., Stutz, E., Thélin, P., Marchant, R. and Steck, A. (1993b): Inverse metamorphic zonation in very low-grade Tibetan Zone series of SE Zanskar and its tectonic consequences (NW India, Himalaya). Schweiz. Mineral. Petrogr. Mitt. 73, 79–89.
- SRIKANTIA, S.V. and BHARGAVA, O.N. (1979): The Tandi Group of Lahaul its geology and relationship with the Central Himalayan Gneiss. J. Geol. Soc. India 20, 531–539.
- SRIKANTIA, S.V. and BHARGAVA, O.N. (1982): An outline of the structure of the area between the Rohtang Pass in Lahaul and the Indus Valley in Ladakh. Geol. Surv. India Misc. Publ. (Calcutta) 41(3), 193–204.
- STÄUBLI, A. (1989): Polyphase metamorphism and the development of the Main Central Thrust. J. metamorphic Geol. 7, 73-93
- morphic Geol. 7, 73–93.

  STECK, A., SPRING, L., VANNAY, J.C., MASSON, H., BUCHER, H., STUTZ, E., MARCHANT, R. and TIÈCHE, J.C. (1993a): Geological transect across the Northwestern Himalaya in eastern Ladakh and Lahul (A model for the continental collision of India and Asia). Eclogae geol. Helv. 86(1), 219–263.
- STECK, A., SPRING, L., VANNAY, J.C., MASSON, H., BUCHER, H., STUTZ, E., MARCHANT, R. and TIÈCHE, J.C. (1993b): The tectonic evolution of the Northwestern Himalaya in eastern Ladakh and Lahul, India. In: TRELOAR, P.J. and SEARLE, M.P. (Eds): Himalayan Tectonics. Geological Society Special Publication (London), 74, 265–276.

- STUTZ, E. (1988): Géologie de la chaîne de Nyimaling aux confins du Ladakh et du Rupshu (NW-Himalaya, Inde) évolution paléogéographique et tectonique d'un segment de la marge nord-indienne. Mém. Géol. (Lausanne) 3.
- STUTZ, E. and STECK, A. (1986): La terminaison occidentale du Cristallin du Tso Morari (Haut-Himalaya; Ladakh méridional, Inde): Subdivision et tectonique de nappe. Eclogae geol. Helv. 79(2), 253–269.
- Thöni, M. (1977): Geology, structural evolution and metamorphic zoning in the Kulu Valley (Himachal Himalayas, India) with special reference to the reversed metamorphism. Mitt. Ges. Geol. Bergbaustud. Osterr. 24, 125–187.
- Treloar, P.J. and Rex, D. (1990): Cooling and uplift histories of the crystalline crust stack of the Indian plate internal zones west of Nanga Parbat, Pakistan Himalaya. Tectonophysics 191, 189–198.
- Vannay, J.C. (1993): Géologie des chaînes du Haut-Himalaya et du Pir Panjal au Haut-Lahul (NW-Himalaya, Inde) Mém. Géol. (Lausanne), 16.
- Vannay, J.C. and Spring, L. (1993): Geochemistry of the continental basalts within the Tethyan Himalaya of Lahul-Spiti and SE Zanskar (NW India). In: Treloar, P.J. and Searle, M.P. (Eds): Himalayan tectonics. Geological Society Special Publication (London), 74, 237–249.

  Vannay, J.C. and Steck, A. (in press): Tectonic evolu-
- Vannay, J.C. and Steck, A. (in press): Tectonic evolution of the High Himalayan Crystalline and of the Tethyan Zone in Upper Lahul (NW Himalaya, India). Tectonics.
- dia). Tectonics.

  VILLA, I. and ODDONE, M. (1988): <sup>39</sup>Ar/<sup>40</sup>Ar ages of Himalayan leucogranites decrease eastward. 4th Himalayan-Karakorum-Tibet Workshop, Lausanne. Abstract volume (p. 16).

Manuscript received August 18, 1994; minor revision accepted January 21, 1995

# **Appendix**

Tab. A1 Representative analysis of garnets and biotites.

# **Garnets**

Sample Analysis #	AS93106 A-6	AS93116 A-7	AS93126 A-6	AS93136 A-1	AS93137 A-4	AS93152 D-17	AS93159 A-13	AS93179 A-7	AS93204 A-4
6:0	27.06	27.22	27.44		27.67	27.52	27.25	27.06	27.27
SiO <sub>2</sub>	37.26	37.32	37.44	37.47	37.67	37.52	37.35	37.06	37.37
TiO <sub>2</sub>	0.15	0.16	0.01	0.00	0.02	0.17	0.01	0.00	0.01
$Al_2O_3$	21.11	21.00	21.02	20.84	21.48	21.08	20.87	20.77	20.56
$Cr_2O_3$	0.01	0.00	0.00	0.01	0.00	0.03	0.01	0.00	0.00
FeO	29.51	22.49	29.43	29.89	24.88	27.98	33.40	34.63	28.20
MgO	0.81	0.24	2.48	2.66	2.70	2.58	3.24	3.09	1.34
CaO	9.13	13.21	5.61	5.63	10.43	8.73	2.94	1.71	7.15
MnO	2.94	5.48	4.09	3.95	3.36	2.23	2.16	3.06	6.14
Total	100.92	99.88	100.08	100.45	100.54	100.33	99.97	100.33	100.76
Cations norma	alized to 12 ox	ygens							
Si	2.976	2.986	2.999	2.995	2.970	2.980	3.001	2.988	2.999
Ti	0.009	0.010	0.000	0.000	0.001	0.010	0.000	0.000	0.000
Al	1.985	1.980	1.984	1.963	1.996	1.974	1.976	1.973	1.944
Cr	0.000	0.000	1.501	0.000	0.000	0.002	0.000	0.000	0.000
Fe*++	0.026	0.024	0.017	0.041	0.033	0.034	0.220	0.039	0.056
Fe <sup>++</sup>				1.057	1.600		2.222	2.297	
	1.945	1.481	1.954	1.957	1.608	1.824			1.836
Mg	0.096	0.028	0.296	0.317	0.317	0.305	0.388	0.372	0.160
Ca	0.782	1.133	0.482	0.482	0.881	0.743	0.253	0.148	0.615
Mn	0.199	0.371	0.278	0.267	0.225	0.150	0.147	0.209	0.417
Sum	8.018	8.013	8.010	8.022	8.031	8.022	8.207	8.026	8.027
X Fe	0.644	0.492	0.649	0.647	0.531	0.604	0.738	0.759	0.606
X Mg	0.032	0.009	0.098	0.105	0.105	0.101	0.129	0.123	0.053
X Ca	0.259	0.376	0.160	0.159	0.291	0.246	0.084	0.049	0.203
X Mn	0.066	0.123	0.100	0.139	0.291	0.050	0.049	0.049	0.203
XMg/XFe	0.049	0.019	0.151	0.162	0.197	0.167	0.175	0.162	0.087
				Biotit	es				
Sample	AS93106	AS93116	AS93126	AS93136	AS93137	AS93152	AS93159	AS93179	AS93204
Sample Analysis #	AS93106 A-6	AS93116 A-7	AS93126 A-6			AS93152 D-17	AS93159 A-13	AS93179 A-7	AS93204 A-4
Analysis # SiO <sub>2</sub>	A-6 35.92	A-7 35.29	A-6 37.03	AS93136 A-1a 36.42	AS93137 A-4 36.63	D-17 36.71	A-13 36.53	A-7 35.86	A-4 36.95
Analysis # SiO <sub>2</sub> TiO <sub>2</sub>	35.92 1.39	A-7 35.29 1.50	A-6 37.03 1.66	AS93136 A-1a 36.42 2.62	AS93137 A-4 36.63 1.94	D-17 36.71 2.20	A-13 36.53 2.63	A-7 35.86 1.50	A-4 36.95 1.99
Analysis # SiO <sub>2</sub>	A-6 35.92	A-7 35.29	A-6 37.03	AS93136 A-1a 36.42	AS93137 A-4 36.63	D-17 36.71	A-13 36.53	A-7 35.86	A-4 36.95
Analysis # SiO <sub>2</sub> TiO <sub>2</sub>	35.92 1.39	35.29 1.50 16.51	A-6 37.03 1.66 17.69	AS93136 A-1a 36.42 2.62 18.02	AS93137 A-4 36.63 1.94 18.09	36.71 2.20 17.75	A-13 36.53 2.63	A-7 35.86 1.50	A-4 36.95 1.99
Analysis # SiO <sub>2</sub> TiO <sub>2</sub> Al <sub>2</sub> O <sub>3</sub> FeO	35.92 1.39 17.31 22.70	A-7 35.29 1.50	37.03 1.66 17.69 17.21	AS93136 A-1a 36.42 2.62 18.02 18.73	AS93137 A-4 36.63 1.94 18.09 18.13	36.71 2.20 17.75 16.78	36.53 2.63 18.97 17.68	35.86 1.50 19.19	36.95 1.99 16.96
Analysis # SiO <sub>2</sub> TiO <sub>2</sub> Al <sub>2</sub> O <sub>3</sub> FeO MgO	35.92 1.39 17.31 22.70 8.37	35.29 1.50 16.51 28.83 3.63	A-6 37.03 1.66 17.69 17.21 11.78	AS93136 A-1a 36.42 2.62 18.02 18.73 9.90	AS93137 A-4 36.63 1.94 18.09 18.13 10.73	D-17  36.71 2.20 17.75 16.78 11.73	36.53 2.63 18.97 17.68 10.51	35.86 1.50 19.19 18.74 10.41	36.95 1.99 16.96 17.80 11.78
Analysis # SiO <sub>2</sub> TiO <sub>2</sub> Al <sub>2</sub> O <sub>3</sub> FeO MgO MnO	35.92 1.39 17.31 22.70 8.37 0.12	A-7 35.29 1.50 16.51 28.83 3.63 0.20	A-6 37.03 1.66 17.69 17.21 11.78 0.03	AS93136 A-1a 36.42 2.62 18.02 18.73 9.90 0.09	AS93137 A-4 36.63 1.94 18.09 18.13 10.73 0.24	36.71 2.20 17.75 16.78 11.73 0.06	36.53 2.63 18.97 17.68 10.51 0.03	A-7 35.86 1.50 19.19 18.74 10.41 0.08	36.95 1.99 16.96 17.80 11.78 0.15
Analysis #  SiO <sub>2</sub> TiO <sub>2</sub> Al <sub>2</sub> O <sub>3</sub> FeO MgO MnO K <sub>2</sub> O	A-6  35.92 1.39 17.31 22.70 8.37 0.12 9.05	35.29 1.50 16.51 28.83 3.63 0.20 9.65	A-6  37.03 1.66 17.69 17.21 11.78 0.03 9.49	AS93136 A-1a 36.42 2.62 18.02 18.73 9.90 0.09 9.35	AS93137 A-4 36.63 1.94 18.09 18.13 10.73 0.24 8.83	36.71 2.20 17.75 16.78 11.73 0.06 9.18	36.53 2.63 18.97 17.68 10.51 0.03 8.93	35.86 1.50 19.19 18.74 10.41 0.08 9.23	A-4  36.95 1.99 16.96 17.80 11.78 0.15 9.22
Analysis # SiO <sub>2</sub> TiO <sub>2</sub> Al <sub>2</sub> O <sub>3</sub> FeO MgO MnO	35.92 1.39 17.31 22.70 8.37 0.12 9.05 0.08	35.29 1.50 16.51 28.83 3.63 0.20 9.65 0.02	A-6  37.03 1.66 17.69 17.21 11.78 0.03 9.49 0.19	AS93136 A-1a 36.42 2.62 18.02 18.73 9.90 0.09 9.35 0.17	AS93137 A-4 36.63 1.94 18.09 18.13 10.73 0.24	36.71 2.20 17.75 16.78 11.73 0.06 9.18 0.12	36.53 2.63 18.97 17.68 10.51 0.03	A-7 35.86 1.50 19.19 18.74 10.41 0.08	A-4 36.95 1.99 16.96 17.80 11.78 0.15 9.22 0.09
Analysis #  SiO <sub>2</sub> TiO <sub>2</sub> Al <sub>2</sub> O <sub>3</sub> FeO MgO MnO K <sub>2</sub> O Na <sub>2</sub> O	35.92 1.39 17.31 22.70 8.37 0.12 9.05 0.08 0.68	35.29 1.50 16.51 28.83 3.63 0.20 9.65 0.02 0.40	A-6  37.03 1.66 17.69 17.21 11.78 0.03 9.49 0.19 0.00	AS93136 A-1a 36.42 2.62 18.02 18.73 9.90 0.09 9.35 0.17 0.00	AS93137 A-4 36.63 1.94 18.09 18.13 10.73 0.24 8.83 0.18 0.37	36.71 2.20 17.75 16.78 11.73 0.06 9.18 0.12 0.18	36.53 2.63 18.97 17.68 10.51 0.03 8.93 0.32 0.18	35.86 1.50 19.19 18.74 10.41 0.08 9.23 0.29 0.00	A-4  36.95 1.99 16.96 17.80 11.78 0.15 9.22 0.09 0.18
Analysis #  SiO <sub>2</sub> TiO <sub>2</sub> Al <sub>2</sub> O <sub>3</sub> FeO MgO MnO K <sub>2</sub> O Na <sub>2</sub> O	35.92 1.39 17.31 22.70 8.37 0.12 9.05 0.08	35.29 1.50 16.51 28.83 3.63 0.20 9.65 0.02	A-6  37.03 1.66 17.69 17.21 11.78 0.03 9.49 0.19	AS93136 A-1a 36.42 2.62 18.02 18.73 9.90 0.09 9.35 0.17	AS93137 A-4 36.63 1.94 18.09 18.13 10.73 0.24 8.83 0.18	36.71 2.20 17.75 16.78 11.73 0.06 9.18 0.12	36.53 2.63 18.97 17.68 10.51 0.03 8.93 0.32	35.86 1.50 19.19 18.74 10.41 0.08 9.23 0.29	A-4 36.95 1.99 16.96 17.80 11.78 0.15 9.22 0.09
Analysis #  SiO <sub>2</sub> TiO <sub>2</sub> Al <sub>2</sub> O <sub>3</sub> FeO MgO MnO K <sub>2</sub> O Na <sub>2</sub> O F	A-6  35.92 1.39 17.31 22.70 8.37 0.12 9.05 0.08 0.68	A-7  35.29 1.50 16.51 28.83 3.63 0.20 9.65 0.02 0.40 96.03	A-6  37.03 1.66 17.69 17.21 11.78 0.03 9.49 0.19 0.00 95.08	AS93136 A-1a 36.42 2.62 18.02 18.73 9.90 0.09 9.35 0.17 0.00 95.29	AS93137 A-4 36.63 1.94 18.09 18.13 10.73 0.24 8.83 0.18 0.37 95.13	36.71 2.20 17.75 16.78 11.73 0.06 9.18 0.12 0.18	A-13  36.53 2.63 18.97 17.68 10.51 0.03 8.93 0.32 0.18	A-7  35.86 1.50 19.19 18.74 10.41 0.08 9.23 0.29 0.00 95.30	A-4  36.95 1.99 16.96 17.80 11.78 0.15 9.22 0.09 0.18 95.10
Analysis #  SiO <sub>2</sub> TiO <sub>2</sub> Al <sub>2</sub> O <sub>3</sub> FeO MgO MnO K <sub>2</sub> O Na <sub>2</sub> O F  O = F	A-6  35.92 1.39 17.31 22.70 8.37 0.12 9.05 0.08 0.68  95.62 0.29	35.29 1.50 16.51 28.83 3.63 0.20 9.65 0.02 0.40 96.03 0.17	A-6  37.03 1.66 17.69 17.21 11.78 0.03 9.49 0.19 0.00 95.08 0.00	AS93136 A-1a 36.42 2.62 18.02 18.73 9.90 0.09 9.35 0.17 0.00 95.29 0.00	AS93137 A-4 36.63 1.94 18.09 18.13 10.73 0.24 8.83 0.18 0.37 95.13 0.16	36.71 2.20 17.75 16.78 11.73 0.06 9.18 0.12 0.18 94.72 0.08	36.53 2.63 18.97 17.68 10.51 0.03 8.93 0.32 0.18 95.77 0.08	35.86 1.50 19.19 18.74 10.41 0.08 9.23 0.29 0.00 95.30 0.00	A-4  36.95 1,99 16.96 17.80 11.78 0.15 9.22 0.09 0.18 95.10 0.08
Analysis #  SiO <sub>2</sub> TiO <sub>2</sub> Al <sub>2</sub> O <sub>3</sub> FeO MgO MnO K <sub>2</sub> O Na <sub>2</sub> O F  O = F  total  Cations normal	A-6  35.92 1.39 17.31 22.70 8.37 0.12 9.05 0.08 0.68 95.62 0.29 95.33	35.29 1.50 16.51 28.83 3.63 0.20 9.65 0.02 0.40 96.03 0.17 95.86	A-6  37.03 1.66 17.69 17.21 11.78 0.03 9.49 0.19 0.00 95.08 0.00	AS93136 A-1a 36.42 2.62 18.02 18.73 9.90 0.09 9.35 0.17 0.00 95.29 0.00	AS93137 A-4 36.63 1.94 18.09 18.13 10.73 0.24 8.83 0.18 0.37 95.13 0.16 94.97	D-17  36.71 2.20 17.75 16.78 11.73 0.06 9.18 0.12 0.18 94.72 0.08	36.53 2.63 18.97 17.68 10.51 0.03 8.93 0.32 0.18 95.77 0.08	A-7  35.86 1.50 19.19 18.74 10.41 0.08 9.23 0.29 0.00 95.30 0.00	A-4  36.95 1,99 16.96 17.80 11.78 0.15 9.22 0.09 0.18 95.10 0.08
Analysis #  SiO <sub>2</sub> TiO <sub>2</sub> Al <sub>2</sub> O <sub>3</sub> FeO MgO MnO K <sub>2</sub> O Na <sub>2</sub> O F  O = F  total  Cations norma	A-6  35.92 1.39 17.31 22.70 8.37 0.12 9.05 0.08 0.68 95.62 0.29 95.33	35.29 1.50 16.51 28.83 3.63 0.20 9.65 0.02 0.40 96.03 0.17 95.86 aivalent O 5.634	A-6  37.03 1.66 17.69 17.21 11.78 0.03 9.49 0.19 0.00 95.08 0.00 95.08	AS93136 A-1a 36.42 2.62 18.02 18.73 9.90 0.09 9.35 0.17 0.00 95.29 0.00 95.29	AS93137 A-4 36.63 1.94 18.09 18.13 10.73 0.24 8.83 0.18 0.37 95.13 0.16 94.97	D-17  36.71 2.20 17.75 16.78 11.73 0.06 9.18 0.12 0.18 94.72 0.08 94.64	A-13  36.53 2.63 18.97 17.68 10.51 0.03 8.93 0.32 0.18 95.77 0.08	A-7  35.86 1.50 19.19 18.74 10.41 0.08 9.23 0.29 0.00 95.30 0.00 95.30	A-4  36.95 1.99 16.96 17.80 11.78 0.15 9.22 0.09 0.18 95.10 0.08  95.02
Analysis #  SiO <sub>2</sub> TiO <sub>2</sub> Al <sub>2</sub> O <sub>3</sub> FeO MgO MnO K <sub>2</sub> O Na <sub>2</sub> O F  O = F  total  Cations normal Si Ti	A-6  35.92 1.39 17.31 22.70 8.37 0.12 9.05 0.08 0.68  95.62 0.29  95.33  dized to 22 equ 5.568 0.161	35.29 1.50 16.51 28.83 3.63 0.20 9.65 0.02 0.40 96.03 0.17 95.86 divalent O 5.634 0.179	A-6  37.03 1.66 17.69 17.21 11.78 0.03 9.49 0.19 0.00 95.08 0.00  95.08	AS93136 A-1a 36.42 2.62 18.02 18.73 9.90 0.09 9.35 0.17 0.00 95.29 0.00 95.29	AS93137 A-4  36.63 1.94 18.09 18.13 10.73 0.24 8.83 0.18 0.37 95.13 0.16  94.97	D-17  36.71 2.20 17.75 16.78 11.73 0.06 9.18 0.12 0.18 94.72 0.08 94.64	A-13  36.53 2.63 18.97 17.68 10.51 0.03 8.93 0.32 0.18 95.77 0.08  95.70	A-7  35.86 1.50 19.19 18.74 10.41 0.08 9.23 0.29 0.00 95.30 0.00  95.30  5.428 0.171	A-4  36.95 1.99 16.96 17.80 11.78 0.15 9.22 0.09 0.18 95.10 0.08  95.02
Analysis #  SiO <sub>2</sub> TiO <sub>2</sub> Al <sub>2</sub> O <sub>3</sub> FeO MgO MnO K <sub>2</sub> O Na <sub>2</sub> O F  O = F  total  Cations normal Si Ti Al	A-6  35.92 1.39 17.31 22.70 8.37 0.12 9.05 0.08 0.68 95.62 0.29 95.33  dized to 22 equ 5.568 0.161 3.162	A-7  35.29 1.50 16.51 28.83 3.63 0.20 9.65 0.02 0.40 96.03 0.17  95.86  divalent O 5.634 0.179 3.104	A-6  37.03 1.66 17.69 17.21 11.78 0.03 9.49 0.19 0.00 95.08 0.00  95.08  5.790 0.188 3.140	AS93136 A-1a 36.42 2.62 18.02 18.73 9.90 0.09 9.35 0.17 0.00 95.29 0.00 95.29 5.517 0.298 3.216	AS93137 A-4  36.63 1.94 18.09 18.13 10.73 0.24 8.83 0.18 0.37 95.13 0.16  94.97	D-17  36.71 2.20 17.75 16.78 11.73 0.06 9.18 0.12 0.18 94.72 0.08 94.64  5.545 0.249 3.159	A-13  36.53 2.63 18.97 17.68 10.51 0.03 8.93 0.32 0.18 95.77 0.08  95.70  5.466 0.296 3.345	A-7  35.86 1.50 19.19 18.74 10.41 0.08 9.23 0.29 0.00 95.30 0.00  95.30  5.428 0.171 3.423	A-4  36.95 1.99 16.96 17.80 11.78 0.15 9.22 0.09 0.18 95.10 0.08  95.02  5.591 0.227 3.024
Analysis #  SiO <sub>2</sub> TiO <sub>2</sub> Al <sub>2</sub> O <sub>3</sub> FeO MgO MnO K <sub>2</sub> O Na <sub>2</sub> O F  O = F  total  Cations norma Si Ti Al Fe	A-6  35.92 1.39 17.31 22.70 8.37 0.12 9.05 0.08 0.68 95.62 0.29 95.33 dized to 22 equ. 5.568 0.161 3.162 2.942	A-7  35.29 1.50 16.51 28.83 3.63 0.20 9.65 0.02 0.40 96.03 0.17  95.86  uivalent O 5.634 0.179 3.104 3.846	A-6  37.03 1.66 17.69 17.21 11.78 0.03 9.49 0.19 0.00 95.08 0.00  95.08  5.790 0.188 3.140 2.168	AS93136 A-1a 36.42 2.62 18.02 18.73 9.90 0.09 9.35 0.17 0.00 95.29 0.00 95.29 5.517 0.298 3.216 2.373	AS93137 A-4  36.63 1.94 18.09 18.13 10.73 0.24 8.83 0.18 0.37 95.13 0.16  94.97  5.546 0.220 3.227 2.295	D-17  36.71 2.20 17.75 16.78 11.73 0.06 9.18 0.12 0.18 94.72 0.08 94.64  5.545 0.249 3.159 2.120	A-13  36.53 2.63 18.97 17.68 10.51 0.03 8.93 0.32 0.18  95.77 0.08  95.70  5.466 0.296 3.345 2.213	A-7  35.86 1.50 19.19 18.74 10.41 0.08 9.23 0.29 0.00 95.30 0.00  95.30 5.428 0.171 3.423 2.373	A-4  36.95 1.99 16.96 17.80 11.78 0.15 9.22 0.09 0.18 95.10 0.08  95.02  5.591 0.227 3.024 2.252
Analysis #  SiO <sub>2</sub> TiO <sub>2</sub> Al <sub>2</sub> O <sub>3</sub> FeO MgO MnO K <sub>2</sub> O Na <sub>2</sub> O F  O = F  total  Cations norma Si Ti Al	A-6  35.92 1.39 17.31 22.70 8.37 0.12 9.05 0.08 0.68 95.62 0.29 95.33  dized to 22 equals 5.568 0.161 3.162 2.942 1.932	35.29 1.50 16.51 28.83 3.63 0.20 9.65 0.02 0.40 96.03 0.17 95.86 aivalent O 5.634 0.179 3.104 3.846 0.863	A-6  37.03 1.66 17.69 17.21 11.78 0.03 9.49 0.19 0.00 95.08 0.00  95.08  5.790 0.188 3.140	AS93136 A-1a 36.42 2.62 18.02 18.73 9.90 0.09 9.35 0.17 0.00 95.29 0.00 95.29 5.517 0.298 3.216 2.373 2.234	AS93137 A-4  36.63 1.94 18.09 18.13 10.73 0.24 8.83 0.18 0.37 95.13 0.16  94.97	D-17  36.71 2.20 17.75 16.78 11.73 0.06 9.18 0.12 0.18 94.72 0.08 94.64  5.545 0.249 3.159	A-13  36.53 2.63 18.97 17.68 10.51 0.03 8.93 0.32 0.18 95.77 0.08  95.70  5.466 0.296 3.345 2.213 2.345	A-7  35.86 1.50 19.19 18.74 10.41 0.08 9.23 0.29 0.00 95.30 0.00  95.30  5.428 0.171 3.423	A-4  36.95 1.99 16.96 17.80 11.78 0.15 9.22 0.09 0.18 95.10 0.08  95.02  5.591 0.227 3.024
Analysis #  SiO <sub>2</sub> TiO <sub>2</sub> Al <sub>2</sub> O <sub>3</sub> FeO MgO MnO K <sub>2</sub> O Na <sub>2</sub> O F  O = F  total  Cations norma Si Ti Al Fe	A-6  35.92 1.39 17.31 22.70 8.37 0.12 9.05 0.08 0.68 95.62 0.29 95.33  dized to 22 equals 5.568 0.161 3.162 2.942 1.932	35.29 1.50 16.51 28.83 3.63 0.20 9.65 0.02 0.40 96.03 0.17 95.86 aivalent O 5.634 0.179 3.104 3.846 0.863	A-6  37.03 1.66 17.69 17.21 11.78 0.03 9.49 0.19 0.00 95.08 0.00  95.08 5.790 0.188 3.140 2.168 2.645	AS93136 A-1a 36.42 2.62 18.02 18.73 9.90 0.09 9.35 0.17 0.00 95.29 0.00 95.29 5.517 0.298 3.216 2.373 2.234	AS93137 A-4  36.63 1.94 18.09 18.13 10.73 0.24 8.83 0.18 0.37 95.13 0.16  94.97  5.546 0.220 3.227 2.295 2.421	D-17  36.71 2.20 17.75 16.78 11.73 0.06 9.18 0.12 0.18 94.72 0.08  94.64  5.545 0.249 3.159 2.120 2.641	A-13  36.53 2.63 18.97 17.68 10.51 0.03 8.93 0.32 0.18 95.77 0.08  95.70  5.466 0.296 3.345 2.213 2.345	A-7  35.86 1.50 19.19 18.74 10.41 0.08 9.23 0.29 0.00 95.30 0.00  95.30 5.428 0.171 3.423 2.373 2.348	A-4  36.95 1.99 16.96 17.80 11.78 0.15 9.22 0.09 0.18 95.10 0.08  95.02  5.591 0.227 3.024 2.252 2.656
Analysis #  SiO <sub>2</sub> TiO <sub>2</sub> Al <sub>2</sub> O <sub>3</sub> FeO MgO MnO K <sub>2</sub> O Na <sub>2</sub> O F  O = F  total  Cations norma Si Ti Al Fe Mg Mn	A-6  35.92 1.39 17.31 22.70 8.37 0.12 9.05 0.08 0.68 95.62 0.29 95.33 dized to 22 equals 5.568 0.161 3.162 2.942 1.932 0.016	A-7  35.29 1.50 16.51 28.83 3.63 0.20 9.65 0.02 0.40 96.03 0.17  95.86  aivalent O 5.634 0.179 3.104 3.846 0.863 0.027	A-6  37.03 1.66 17.69 17.21 11.78 0.03 9.49 0.19 0.00 95.08 0.00  95.08  5.790 0.188 3.140 2.168 2.645 0.004	AS93136 A-1a 36.42 2.62 18.02 18.73 9.90 0.09 9.35 0.17 0.00 95.29 0.00 95.29 5.517 0.298 3.216 2.373 2.234 0.012	AS93137 A-4  36.63 1.94 18.09 18.13 10.73 0.24 8.83 0.18 0.37 95.13 0.16  94.97  5.546 0.220 3.227 2.295 2.421 0.031	D-17  36.71 2.20 17.75 16.78 11.73 0.06 9.18 0.12 0.18 94.72 0.08  94.64  5.545 0.249 3.159 2.120 2.641 0.007	A-13  36.53 2.63 18.97 17.68 10.51 0.03 8.93 0.32 0.18 95.77 0.08  95.70  5.466 0.296 3.345 2.213 2.345 0.004	A-7  35.86 1.50 19.19 18.74 10.41 0.08 9.23 0.29 0.00 95.30 0.00  95.30 5.428 0.171 3.423 2.373 2.348 0.011	A-4  36.95 1.99 16.96 17.80 11.78 0.15 9.22 0.09 0.18 95.10 0.08  95.02  5.591 0.227 3.024 2.252 2.656 0.019
Analysis #  SiO <sub>2</sub> TiO <sub>2</sub> Al <sub>2</sub> O <sub>3</sub> FeO MgO MnO K <sub>2</sub> O Na <sub>2</sub> O F  O = F  total  Cations norma Si Ti Al Fe Mg Mn K	A-6  35.92 1.39 17.31 22.70 8.37 0.12 9.05 0.08 0.68 95.62 0.29 95.33 dized to 22 equ. 5.568 0.161 3.162 2.942 1.932 0.016 1.790	A-7  35.29 1.50 16.51 28.83 3.63 0.20 9.65 0.02 0.40 96.03 0.17  95.86  aivalent O 5.634 0.179 3.104 3.846 0.863 0.027 1.965	A-6  37.03 1.66 17.69 17.21 11.78 0.03 9.49 0.19 0.00 95.08 0.00  95.08  5.790 0.188 3.140 2.168 2.645 0.004 1.823	AS93136 A-1a 36.42 2.62 18.02 18.73 9.90 0.09 9.35 0.17 0.00 95.29 0.00 95.29 5.517 0.298 3.216 2.373 2.234 0.012 1.807	AS93137 A-4  36.63 1.94 18.09 18.13 10.73 0.24 8.83 0.18 0.37 95.13 0.16  94.97  5.546 0.220 3.227 2.295 2.421 0.031 1.706	D-17  36.71 2.20 17.75 16.78 11.73 0.06 9.18 0.12 0.18 94.72 0.08  94.64  5.545 0.249 3.159 2.120 2.641 0.007 1.769	A-13  36.53 2.63 18.97 17.68 10.51 0.03 8.93 0.32 0.18 95.77 0.08  95.70  5.466 0.296 3.345 2.213 2.345 0.004 1.704	A-7  35.86 1.50 19.19 18.74 10.41 0.08 9.23 0.29 0.00 95.30 0.00  95.30 5.428 0.171 3.423 2.373 2.348 0.011 1.782	A-4  36.95 1.99 16.96 17.80 11.78 0.15 9.22 0.09 0.18 95.10 0.08  95.02  5.591 0.227 3.024 2.252 2.656 0.019 0.086
Analysis #  SiO <sub>2</sub> TiO <sub>2</sub> Al <sub>2</sub> O <sub>3</sub> FeO MgO MnO K <sub>2</sub> O Na <sub>2</sub> O F  O = F  total  Cations norma Si Ti Al Fe Mg Mn	A-6  35.92 1.39 17.31 22.70 8.37 0.12 9.05 0.08 0.68 95.62 0.29 95.33 dized to 22 equals 5.568 0.161 3.162 2.942 1.932 0.016	A-7  35.29 1.50 16.51 28.83 3.63 0.20 9.65 0.02 0.40 96.03 0.17  95.86  aivalent O 5.634 0.179 3.104 3.846 0.863 0.027	A-6  37.03 1.66 17.69 17.21 11.78 0.03 9.49 0.19 0.00 95.08 0.00  95.08  5.790 0.188 3.140 2.168 2.645 0.004	AS93136 A-1a 36.42 2.62 18.02 18.73 9.90 0.09 9.35 0.17 0.00 95.29 0.00 95.29 5.517 0.298 3.216 2.373 2.234 0.012	AS93137 A-4  36.63 1.94 18.09 18.13 10.73 0.24 8.83 0.18 0.37 95.13 0.16  94.97  5.546 0.220 3.227 2.295 2.421 0.031	D-17  36.71 2.20 17.75 16.78 11.73 0.06 9.18 0.12 0.18 94.72 0.08  94.64  5.545 0.249 3.159 2.120 2.641 0.007	A-13  36.53 2.63 18.97 17.68 10.51 0.03 8.93 0.32 0.18 95.77 0.08  95.70  5.466 0.296 3.345 2.213 2.345 0.004	A-7  35.86 1.50 19.19 18.74 10.41 0.08 9.23 0.29 0.00 95.30 0.00  95.30 5.428 0.171 3.423 2.373 2.348 0.011	A-4  36.95 1.99 16.96 17.80 11.78 0.15 9.22 0.09 0.18 95.10 0.08  95.02  5.591 0.227 3.024 2.252 2.656 0.019

# Garnets (cont.)

AS93205A A-6	AS93214 B-4	AS93218 A-8	AS93221 A-3	AS93225 A-2	AS93241 A-17	AS93247B B-8	AS93252 B-4	AS93254 A-2	AS93259 B-30	AS93260 D-10
37.39 0.00	36.95 0.03	37.09 0.00	37.48 0.08	37.34 0.05	37.88 0.03	36.56 0.03	37.08 0.06	37.15 0.11	37.18 0.03	36.77 0.03
20.96	20.94	20.98	21.46	21.11	21.41	21.11	20.97	20.77	21.42	21.20
0.00	0.01	0.07	0.04	0.01	0.03	0.02	0.05	0.06	0.02	0.02
34.51	27.30	33.82	27.14	31.41	30.32	33.01	32.49	29.58	34.04	33.70
3.45	1.27	3.55	3.28	3.21	4.74	2.35	2.27	2.14	3.54	2.18
1.57 3.08	7.37 5.85	3.53 1.46	7.36 3.70	3.47 3.97	3.15 2.99	3.43 4.23	3.53 4.24	5.81 4.92	2.44 2.13	1.92 5.08
				6.						
100.95	99.72	100.50	100.52	100.57	100.55	100.73	100.70	100.53	100.79	100.89
2.989	2.985	2.968	2.966	2.983	2.990	2.947	2.980	2.981	2.965	2.964
0.000	0.002	0.000	0.004	0.003	0.002	0.002	0.004	0.006	0.002	0.001
1.975	1.994	1.979	2.001	1.987	1.992	2.005	1.987	1.964	2.013	2.014
0.000	0.000	0.004	0.002	0.000	0.002	0.002	0.003	0.004	0.001	0.001
0.036	0.019	0.048	0.026	0.026	0.015	0.044	0.027	0.045	0.018	0.019
2.270	1.825	2.215	1.769	2.072	1.987	2.181	2.157	1.940	2.252	2.252
0.411	0.152	0.423	0.387	0.382	0.558	0.282 0.296	0.272	0.255	0.421	0.261
0.134 0.209	0.638 0.400	0.302 0.099	0.624 0.248	0.297 0.269	0.267 0.200	0.296	0.304 0.289	0.499 0.335	0.208 0.144	0.166 0.347
8.024	8.015	8.038	8.027	8.019	8.013	8.048	8.023	8.029	8.024	8.025
0.751 0.136	0.605	0.729 $0.139$	0.584 0.128	0.686 0.126	0.660 0.185	$0.716 \\ 0.093$	$0.714 \\ 0.090$	0.640 0.084	0.744 0.139	0.744 0.086
0.136	$0.050 \\ 0.212$	0.139	0.128	0.126	0.183	0.093	0.090	0.064	0.139	0.055
0.044	0.212	0.033	0.280	0.089	0.066	0.095	0.096	0.103	0.048	0.115
0.181	0.083	0.191	0.219	0.184	0.281	0.129	0.126	0.131	0.187	0.116
0.101	0.005	0.171	0.217	0.104	0.201	0.123	0.120	0.151	0.107	0.110
				Bioti	ites (con	t.)				
AS93205A A-6a	AS93214 B-4	AS93218 A-8	AS93221 A-3	Bioti AS93225 A-2		AS93247B B-8	AS93252 B-4	AS93254 A-2	AS93259 B-30	AS93260 D-10
A-6a	B-4	A-8	A-3	AS93225 A-2	AS93241 A-17	AS93247B B-8	B-4	A-2	B-30	D-10
A-6a 36.76 1.51		A-8 36.23		AS93225 A-2 36.22	AS93241 A-17 37.03 1.47	AS93247B B-8 35.28 1.63	B-4 35.41	A-2 36.57		D-10 35.23 1.80
36.76 1.51 19.17	35.93 2.17 17.41	A-8 36.23 1.38 17.72	37.23 1.79 17.47	AS93225 A-2 36.22 1.98 17.82	AS93241 A-17 37.03 1.47 19.02	AS93247B B-8 35.28 1.63 18.92	35.41 1.73 18.55	36.57 1.83 17.67	36.47 1.83 18.94	D-10 35.23 1.80 17.97
A-6a  36.76 1.51 19.17 17.15	35.93 2.17 17.41 20.68	A-8 36.23 1.38 17.72 18.35	37.23 1.79 17.47 16.20	AS93225 A-2 36.22 1.98 17.82 18.76	AS93241 A-17 37.03 1.47 19.02 13.97	AS93247B B-8 35,28 1,63 18,92 20,00	35.41 1.73 18.55 21.08	A-2 36.57 1.83 17.67 19.19	36.47 1.83 18.94 16.56	D-10 35.23 1.80 17.97 21.80
A-6a  36.76 1.51 19.17 17.15 11.69	35.93 2.17 17.41 20.68 9.48	A-8  36.23 1.38 17.72 18.35 11.21	37.23 1.79 17.47 16.20 12.60	AS93225 A-2 36.22 1.98 17.82 18.76 10.47	AS93241 A-17 37.03 1.47 19.02 13.97 14.09	AS93247B B-8 35.28 1.63 18.92 20.00 9.12	35.41 1.73 18.55 21.08 9.16	36.57 1.83 17.67 19.19 10.78	36.47 1.83 18.94 16.56 12.01	D-10 35.23 1.80 17.97 21.80 9.17
A-6a  36.76 1.51 19.17 17.15 11.69 0.06	35.93 2.17 17.41 20.68 9.48 0.21	A-8 36.23 1.38 17.72 18.35 11.21 0.09	A-3 37.23 1.79 17.47 16.20 12.60 0.08	AS93225 A-2 36.22 1.98 17.82 18.76 10.47 0.22	AS93241 A-17 37.03 1.47 19.02 13.97 14.09 0.08	AS93247B B-8 35.28 1.63 18.92 20.00 9.12 0.20	35.41 1.73 18.55 21.08 9.16 0.12	36.57 1.83 17.67 19.19 10.78 0.13	36.47 1.83 18.94 16.56 12.01 0.00	D-10  35.23 1.80 17.97 21.80 9.17 0.10
A-6a  36.76 1.51 19.17 17.15 11.69 0.06 8.55	B-4 35.93 2.17 17.41 20.68 9.48 0.21 9.27	A-8 36.23 1.38 17.72 18.35 11.21 0.09 9.27	A-3 37.23 1.79 17.47 16.20 12.60 0.08 9.38	AS93225 A-2 36.22 1.98 17.82 18.76 10.47 0.22 9.60	AS93241 A-17 37.03 1.47 19.02 13.97 14.09 0.08 8.49	AS93247B B-8 35.28 1.63 18.92 20.00 9.12 0.20 9.15	35.41 1.73 18.55 21.08 9.16 0.12 9.50	A-2  36.57 1.83 17.67 19.19 10.78 0.13 9.05	36.47 1.83 18.94 16.56 12.01 0.00 8.56	D-10 35.23 1.80 17.97 21.80 9.17 0.10 9.06
A-6a  36.76 1.51 19.17 17.15 11.69 0.06 8.55 0.36	B-4 35.93 2.17 17.41 20.68 9.48 0.21 9.27 0.13	A-8  36.23 1.38 17.72 18.35 11.21 0.09 9.27 0.10	A-3 37.23 1.79 17.47 16.20 12.60 0.08 9.38 0.15	AS93225 A-2 36.22 1.98 17.82 18.76 10.47 0.22 9.60 0.16	AS93241 A-17 37.03 1.47 19.02 13.97 14.09 0.08 8.49 0.46	AS93247B B-8 35.28 1.63 18.92 20.00 9.12 0.20 9.15 0.12	35.41 1.73 18.55 21.08 9.16 0.12 9.50 0.19	36.57 1.83 17.67 19.19 10.78 0.13 9.05 0.11	36.47 1.83 18.94 16.56 12.01 0.00 8.56 0.41	35.23 1.80 17.97 21.80 9.17 0.10 9.06 0.16
A-6a  36.76 1.51 19.17 17.15 11.69 0.06 8.55 0.36 0.00	B-4 35.93 2.17 17.41 20.68 9.48 0.21 9.27 0.13 0.73	A-8  36.23 1.38 17.72 18.35 11.21 0.09 9.27 0.10 0.19	A-3  37.23 1.79 17.47 16.20 12.60 0.08 9.38 0.15 0.27	AS93225 A-2 36.22 1.98 17.82 18.76 10.47 0.22 9.60 0.16 0.14	AS93241 A-17 37.03 1.47 19.02 13.97 14.09 0.08 8.49 0.46 0.02	AS93247B B-8 35,28 1,63 18,92 20,00 9,12 0,20 9,15 0,12 0,24	35.41 1.73 18.55 21.08 9.16 0.12 9.50 0.19 0.22	A-2  36.57 1.83 17.67 19.19 10.78 0.13 9.05 0.11 0.06	B-30 36.47 1.83 18.94 16.56 12.01 0.00 8.56 0.41 0.39	D-10 35.23 1.80 17.97 21.80 9.17 0.10 9.06 0.16 0.20
A-6a  36.76 1.51 19.17 17.15 11.69 0.06 8.55 0.36 0.00 95.26	B-4 35.93 2.17 17.41 20.68 9.48 0.21 9.27 0.13 0.73 96.01	A-8  36.23 1.38 17.72 18.35 11.21 0.09 9.27 0.10 0.19 94.54	A-3  37.23 1.79 17.47 16.20 12.60 0.08 9.38 0.15 0.27	AS93225 A-2 36.22 1.98 17.82 18.76 10.47 0.22 9.60 0.16 0.14 95.37	AS93241 A-17 37.03 1.47 19.02 13.97 14.09 0.08 8.49 0.46 0.02 94.62	AS93247B B-8 35.28 1.63 18.92 20.00 9.12 0.20 9.15 0.12 0.24 94.66	B-4  35.41 1.73 18.55 21.08 9.16 0.12 9.50 0.19 0.22 95.97	A-2  36.57 1.83 17.67 19.19 10.78 0.13 9.05 0.11 0.06 95.38	B-30 36.47 1.83 18.94 16.56 12.01 0.00 8.56 0.41 0.39 95.16	D-10 35.23 1.80 17.97 21.80 9.17 0.10 9.06 0.16 0.20 95.49
A-6a  36.76 1.51 19.17 17.15 11.69 0.06 8.55 0.36 0.00	B-4 35.93 2.17 17.41 20.68 9.48 0.21 9.27 0.13 0.73	A-8  36.23 1.38 17.72 18.35 11.21 0.09 9.27 0.10 0.19	A-3  37.23 1.79 17.47 16.20 12.60 0.08 9.38 0.15 0.27	AS93225 A-2 36.22 1.98 17.82 18.76 10.47 0.22 9.60 0.16 0.14	AS93241 A-17 37.03 1.47 19.02 13.97 14.09 0.08 8.49 0.46 0.02	AS93247B B-8 35,28 1,63 18,92 20,00 9,12 0,20 9,15 0,12 0,24	35.41 1.73 18.55 21.08 9.16 0.12 9.50 0.19 0.22	A-2  36.57 1.83 17.67 19.19 10.78 0.13 9.05 0.11 0.06	B-30 36.47 1.83 18.94 16.56 12.01 0.00 8.56 0.41 0.39	D-10 35.23 1.80 17.97 21.80 9.17 0.10 9.06 0.16 0.20
A-6a  36.76 1.51 19.17 17.15 11.69 0.06 8.55 0.36 0.00 95.26	B-4 35.93 2.17 17.41 20.68 9.48 0.21 9.27 0.13 0.73	A-8  36.23 1.38 17.72 18.35 11.21 0.09 9.27 0.10 0.19 94.54	A-3  37.23 1.79 17.47 16.20 12.60 0.08 9.38 0.15 0.27	AS93225 A-2 36.22 1.98 17.82 18.76 10.47 0.22 9.60 0.16 0.14 95.37	AS93241 A-17 37.03 1.47 19.02 13.97 14.09 0.08 8.49 0.46 0.02 94.62	AS93247B B-8 35.28 1.63 18.92 20.00 9.12 0.20 9.15 0.12 0.24 94.66	B-4  35.41 1.73 18.55 21.08 9.16 0.12 9.50 0.19 0.22 95.97	A-2  36.57 1.83 17.67 19.19 10.78 0.13 9.05 0.11 0.06 95.38	B-30 36.47 1.83 18.94 16.56 12.01 0.00 8.56 0.41 0.39 95.16	D-10 35.23 1.80 17.97 21.80 9.17 0.10 9.06 0.16 0.20 95.49
A-6a  36.76 1.51 19.17 17.15 11.69 0.06 8.55 0.36 0.00 95.26 0.00	B-4  35.93 2.17 17.41 20.68 9.48 0.21 9.27 0.13 0.73 96.01 0.31	A-8  36.23 1.38 17.72 18.35 11.21 0.09 9.27 0.10 0.19 94.54 0.08	A-3  37.23 1.79 17.47 16.20 12.60 0.08 9.38 0.15 0.27 95.16 0.12	AS93225 A-2 36.22 1.98 17.82 18.76 10.47 0.22 9.60 0.16 0.14 95.37 0.06	AS93241 A-17 37.03 1.47 19.02 13.97 14.09 0.08 8.49 0.46 0.02 94.62 0.01	AS93247B B-8 35.28 1.63 18.92 20.00 9.12 0.20 9.15 0.12 0.24 94.66 0.10	35.41 1.73 18.55 21.08 9.16 0.12 9.50 0.19 0.22 95.97 0.09	36.57 1.83 17.67 19.19 10.78 0.13 9.05 0.11 0.06 95.38 0.02	B-30  36.47 1.83 18.94 16.56 12.01 0.00 8.56 0.41 0.39 95.16 0.17	D-10  35.23 1.80 17.97 21.80 9.17 0.10 9.06 0.16 0.20 95.49 0.08
A-6a  36.76 1.51 19.17 17.15 11.69 0.06 8.55 0.36 0.00 95.26 0.00 95.26	B-4  35.93 2.17 17.41 20.68 9.48 0.21 9.27 0.13 0.73 96.01 0.31 95.70	A-8  36.23 1.38 17.72 18.35 11.21 0.09 9.27 0.10 0.19 94.54 0.08	A-3  37.23 1.79 17.47 16.20 12.60 0.08 9.38 0.15 0.27 95.16 0.12 95.05	AS93225 A-2 36.22 1.98 17.82 18.76 10.47 0.22 9.60 0.16 0.14 95.37 0.06 95.31	AS93241 A-17 37.03 1.47 19.02 13.97 14.09 0.08 8.49 0.46 0.02 94.62 0.01	AS93247B B-8 35.28 1.63 18.92 20.00 9.12 0.20 9.15 0.12 0.24 94.66 0.10	35.41 1.73 18.55 21.08 9.16 0.12 9.50 0.19 0.22 95.97 0.09	36.57 1.83 17.67 19.19 10.78 0.13 9.05 0.11 0.06 95.38 0.02	B-30  36.47 1.83 18.94 16.56 12.01 0.00 8.56 0.41 0.39 95.16 0.17	D-10  35.23 1.80 17.97 21.80 9.17 0.10 9.06 0.16 0.20 95.49 0.08
A-6a  36.76 1.51 19.17 17.15 11.69 0.06 8.55 0.36 0.00 95.26 0.00 95.26  5.490 0.170	B-4  35.93 2.17 17.41 20.68 9.48 0.21 9.27 0.13 0.73 96.01 0.31 95.70  5.508 0.249	A-8  36.23 1.38 17.72 18.35 11.21 0.09 9.27 0.10 0.19 94.54 0.08 94.47  5.535 0.159	A-3  37.23 1.79 17.47 16.20 12.60 0.08 9.38 0.15 0.27 95.16 0.12 95.05	AS93225 A-2 36.22 1.98 17.82 18.76 10.47 0.22 9.60 0.16 0.14 95.37 0.06 95.31	AS93241 A-17 37.03 1.47 19.02 13.97 14.09 0.08 8.49 0.46 0.02 94.62 0.01	AS93247B B-8 35.28 1.63 18.92 20.00 9.12 0.20 9.15 0.12 0.24 94.66 0.10 94.56	B-4  35.41 1.73 18.55 21.08 9.16 0.12 9.50 0.19 0.22 95.97 0.09 95.87  5.160 0.199	A-2  36.57 1.83 17.67 19.19 10.78 0.13 9.05 0.11 0.06 95.38 0.02 95.36	B-30  36.47 1.83 18.94 16.56 12.01 0.00 8.56 0.41 0.39 95.16 0.17 95.00  5.467 0.206	D-10  35.23 1.80 17.97 21.80 9.17 0.10 9.06 0.16 0.20 95.49 0.08
A-6a  36.76 1.51 19.17 17.15 11.69 0.06 8.55 0.36 0.00 95.26 0.00 95.26  5.490 0.170 3.374	B-4  35.93 2.17 17.41 20.68 9.48 0.21 9.27 0.13 0.73 96.01 0.31 95.70  5.508 0.249 3.144	A-8  36.23 1.38 17.72 18.35 11.21 0.09 9.27 0.10 0.19 94.54 0.08 94.47  5.535 0.159 3.191	A-3  37.23 1.79 17.47 16.20 12.60 0.08 9.38 0.15 0.27  95.16 0.12  95.05	AS93225 A-2 1.98 17.82 18.76 10.47 0.22 9.60 0.16 0.14 95.37 0.06 95.31	AS93241 A-17 37.03 1.47 19.02 13.97 14.09 0.08 8.49 0.46 0.02 94.62 0.01 94.61 5.486 0.164 3.320	AS93247B B-8 35.28 1.63 18.92 20.00 9.12 0.20 9.15 0.12 0.24 94.66 0.10 94.56	B-4  35.41 1.73 18.55 21.08 9.16 0.12 9.50 0.19 0.22 95.97 0.09 95.87  5.160 0.199 3.343	A-2  36.57 1.83 17.67 19.19 10.78 0.13 9.05 0.11 0.06 95.38 0.02 95.36  5.540 0.208 3.155	B-30  36.47 1.83 18.94 16.56 12.01 0.00 8.56 0.41 0.39 95.16 0.17 95.00  5.467 0.206 3.345	D-10  35.23 1.80 17.97 21.80 9.17 0.10 9.06 0.16 0.20 95.49 0.08  95.40  5.427 0.208 3.261
A-6a  36.76 1.51 19.17 17.15 11.69 0.06 8.55 0.36 0.00 95.26 0.00 95.26  5.490 0.170 3.374 2.142	B-4  35.93 2.17 17.41 20.68 9.48 0.21 9.27 0.13 0.73 96.01 0.31  95.70  5.508 0.249 3.144 2.651	A-8  36.23 1.38 17.72 18.35 11.21 0.09 9.27 0.10 0.19 94.54 0.08 94.47  5.535 0.159 3.191 2.344	A-3  37.23 1.79 17.47 16.20 12.60 0.08 9.38 0.15 0.27 95.16 0.12  95.05  5.590 0.202 3.090 2.034	AS93225 A-2 1.98 17.82 18.76 10.47 0.22 9.60 0.16 0.14 95.37 0.06 95.31 5.508 0.226 3.193 2.386	AS93241 A-17 37.03 1.47 19.02 13.97 14.09 0.08 8.49 0.46 0.02 94.62 0.01 94.61 5.486 0.164 3.320 1.730	AS93247B B-8 35.28 1.63 18.92 20.00 9.12 0.20 9.15 0.12 0.24 94.66 0.10 94.56 5.431 0.189 3.433 2.575	B-4  35.41 1.73 18.55 21.08 9.16 0.12 9.50 0.19 0.22 95.97 0.09  95.87  5.160 0.199 3.343 2.696	A-2  36.57 1.83 17.67 19.19 10.78 0.13 9.05 0.11 0.06 95.38 0.02 95.36  5.540 0.208 3.155 2.432	B-30  36.47 1.83 18.94 16.56 12.01 0.00 8.56 0.41 0.39 95.16 0.17 95.00  5.467 0.206 3.345 2.076	D-10  35.23 1.80 17.97 21.80 9.17 0.10 9.06 0.16 0.20 95.49 0.08  95.40  5.427 0.208 3.261 2.808
A-6a  36.76 1.51 19.17 17.15 11.69 0.06 8.55 0.36 0.00 95.26 0.00 95.26  5.490 0.170 3.374 2.142 2.602	8-4 35.93 2.17 17.41 20.68 9.48 0.21 9.27 0.13 0.73 96.01 0.31 95.70 5.508 0.249 3.144 2.651 2.165	A-8  36.23 1.38 17.72 18.35 11.21 0.09 9.27 0.10 0.19 94.54 0.08  94.47  5.535 0.159 3.191 2.344 2.552	A-3  37.23 1.79 17.47 16.20 12.60 0.08 9.38 0.15 0.27 95.16 0.12  95.05  5.590 0.202 3.090 2.034 2.818	AS93225 A-2 36.22 1.98 17.82 18.76 10.47 0.22 9.60 0.16 0.14 95.37 0.06 95.31 5.508 0.226 3.193 2.386 2.372	AS93241 A-17 37.03 1.47 19.02 13.97 14.09 0.08 8.49 0.46 0.02 94.62 0.01 94.61 5.486 0.164 3.320 1.730 3.111	AS93247B B-8 35.28 1.63 18.92 20.00 9.12 0.20 9.15 0.12 0.24 94.66 0.10 94.56	8-4 35.41 1.73 18.55 21.08 9.16 0.12 9.50 0.19 0.22 95.97 0.09 95.87  5.160 0.199 3.343 2.696 2.088	A-2  36.57 1.83 17.67 19.19 10.78 0.13 9.05 0.11 0.06 95.38 0.02 95.36  5.540 0.208 3.155 2.432 2.434	B-30  36.47 1.83 18.94 16.56 12.01 0.00 8.56 0.41 0.39 95.16 0.17  95.00  5.467 0.206 3.345 2.076 2.682	D-10  35.23 1.80 17.97 21.80 9.17 0.10 9.06 0.16 0.20 95.49 0.08  95.40  5.427 0.208 3.261 2.808 2.104
A-6a  36.76 1.51 19.17 17.15 11.69 0.06 8.55 0.36 0.00 95.26 0.00 95.26  5.490 0.170 3.374 2.142 2.602 0.008	8-4 35.93 2.17 17.41 20.68 9.48 0.21 9.27 0.13 0.73 96.01 0.31 95.70 5.508 0.249 3.144 2.651 2.165 0.028	A-8  36.23 1.38 17.72 18.35 11.21 0.09 9.27 0.10 0.19 94.54 0.08  94.47  5.535 0.159 3.191 2.344 2.552 0.012	A-3  37.23 1.79 17.47 16.20 12.60 0.08 9.38 0.15 0.27 95.16 0.12  95.05  5.590 0.202 3.090 2.034 2.818 0.010	AS93225 A-2 36.22 1.98 17.82 18.76 10.47 0.22 9.60 0.16 0.14 95.37 0.06 95.31 5.508 0.226 3.193 2.386 2.372 0.029	AS93241 A-17 37.03 1.47 19.02 13.97 14.09 0.08 8.49 0.46 0.02 94.62 0.01 94.61 5.486 0.164 3.320 1.730 3.111 0.011	AS93247B B-8 35.28 1.63 18.92 20.00 9.12 0.20 9.15 0.12 0.24 94.66 0.10 94.56 5.431 0.189 3.433 2.575 2.092 0.026	8-4  35.41 1.73 18.55 21.08 9.16 0.12 9.50 0.19 0.22 95.97 0.09  95.87  5.160 0.199 3.343 2.696 2.088 0.016	A-2  36.57 1.83 17.67 19.19 10.78 0.13 9.05 0.11 0.06 95.38 0.02  95.36  5.540 0.208 3.155 2.432 2.434 0.017	B-30  36.47 1.83 18.94 16.56 12.01 0.00 8.56 0.41 0.39 95.16 0.17 95.00  5.467 0.206 3.345 2.076 2.682 0.000	D-10  35.23 1.80 17.97 21.80 9.17 0.10 9.06 0.16 0.20 95.49 0.08  95.40  5.427 0.208 3.261 2.808 2.104 0.013
A-6a  36.76 1.51 19.17 17.15 11.69 0.06 8.55 0.36 0.00 95.26 0.00 95.26  5.490 0.170 3.374 2.142 2.602 0.008 1.628	8-4 35.93 2.17 17.41 20.68 9.48 0.21 9.27 0.13 0.73 96.01 0.31 95.70  5.508 0.249 3.144 2.651 2.165 0.028 1.812	A-8  36.23 1.38 17.72 18.35 11.21 0.09 9.27 0.10 0.19 94.54 0.08  94.47  5.535 0.159 3.191 2.344 2.552 0.012 1.807	A-3  37.23 1.79 17.47 16.20 12.60 0.08 9.38 0.15 0.27 95.16 0.12 95.05  5.590 0.202 3.090 2.034 2.818 0.010 1.797	AS93225 A-2  36.22 1.98 17.82 18.76 10.47 0.22 9.60 0.16 0.14 95.37 0.06  95.31  5.508 0.226 3.193 2.386 2.372 0.029 1.863	AS93241 A-17 37.03 1.47 19.02 13.97 14.09 0.08 8.49 0.46 0.02 94.62 0.01 94.61 5.486 0.164 3.320 1.730 3.111 0.011 1.604	AS93247B B-8 35,28 1,63 18,92 20,00 9,12 0,20 9,15 0,12 0,24 94,66 0,10 94,56 5,431 0,189 3,433 2,575 2,092 0,026 1,797	8-4  35.41 1.73 18.55 21.08 9.16 0.12 9.50 0.19 0.22 95.97 0.09  95.87  5.160 0.199 3.343 2.696 2.088 0.016 1.854	A-2  36.57 1.83 17.67 19.19 10.78 0.13 9.05 0.11 0.06 95.38 0.02  95.36  5.540 0.208 3.155 2.432 2.434 0.017 1.748	B-30  36.47 1.83 18.94 16.56 12.01 0.00 8.56 0.41 0.39 95.16 0.17 95.00  5.467 0.206 3.345 2.076 2.682 0.000 1.638	D-10  35.23 1.80 17.97 21.80 9.17 0.10 9.06 0.16 0.20 95.49 0.08  95.40  5.427 0.208 3.261 2.808 2.104 0.013 1.780
A-6a  36.76 1.51 19.17 17.15 11.69 0.06 8.55 0.36 0.00 95.26 0.00 95.26  5.490 0.170 3.374 2.142 2.602 0.008	8-4 35.93 2.17 17.41 20.68 9.48 0.21 9.27 0.13 0.73 96.01 0.31 95.70 5.508 0.249 3.144 2.651 2.165 0.028	A-8  36.23 1.38 17.72 18.35 11.21 0.09 9.27 0.10 0.19 94.54 0.08  94.47  5.535 0.159 3.191 2.344 2.552 0.012	A-3  37.23 1.79 17.47 16.20 12.60 0.08 9.38 0.15 0.27 95.16 0.12  95.05  5.590 0.202 3.090 2.034 2.818 0.010	AS93225 A-2 36.22 1.98 17.82 18.76 10.47 0.22 9.60 0.16 0.14 95.37 0.06 95.31 5.508 0.226 3.193 2.386 2.372 0.029	AS93241 A-17 37.03 1.47 19.02 13.97 14.09 0.08 8.49 0.46 0.02 94.62 0.01 94.61 5.486 0.164 3.320 1.730 3.111 0.011	AS93247B B-8 35.28 1.63 18.92 20.00 9.12 0.20 9.15 0.12 0.24 94.66 0.10 94.56 5.431 0.189 3.433 2.575 2.092 0.026	8-4  35.41 1.73 18.55 21.08 9.16 0.12 9.50 0.19 0.22 95.97 0.09  95.87  5.160 0.199 3.343 2.696 2.088 0.016	A-2  36.57 1.83 17.67 19.19 10.78 0.13 9.05 0.11 0.06 95.38 0.02  95.36  5.540 0.208 3.155 2.432 2.434 0.017	B-30  36.47 1.83 18.94 16.56 12.01 0.00 8.56 0.41 0.39 95.16 0.17 95.00  5.467 0.206 3.345 2.076 2.682 0.000	D-10  35.23 1.80 17.97 21.80 9.17 0.10 9.06 0.16 0.20 95.49 0.08  95.40  5.427 0.208 3.261 2.808 2.104 0.013

Tab. A2 Representative analyses of garnets and hornblendes.

*Tab. A3* Representative analyses of garnets and plagioclases.

			Garnets						Gai	rnets
ample .nalysis #	AS93126 J-98	AS93152 D-21	AS93204 B-19	AS93221 D-20	AS93254 F-36	AS93274 A-7	3	Sample Analysis #	AS93159 B-22	AS93242 A-9
iO₂ ĭO₂	37.15 0.06	37.35 0.06	37.28 0.05	37.32 0.00	37.27 0.05	37.62 0.13		SiO <sub>2</sub> TiO <sub>2</sub>	37.13 0.00	37.92 0.01
Al <sub>2</sub> Ō <sub>3</sub> Cr <sub>2</sub> O <sub>3</sub>	$\frac{20.98}{0.10}$	$\frac{21.28}{0.00}$	20.73 0.04	21.58 0.01	20.81 0.00	21.05 0.02		$ ext{Al}_2 ilde{ ext{O}}_3 \  ext{Cr}_2 ext{O}_3$	20.90 0.00	21.38 0.04
TeO MgO CaO	31.23 2.66 5.45	27.94 2.54 8.63	27.53 1.30 7.80	26.00 3.08 7.72	26.68 1.96 8.30	23.69 1.89 8.67		FeO MgO CaO	33.99 3.30 2.62	30.32 5.14 2.89
<b>InO</b>	2.30	2.29	5.92	4.78	4.81	7.71		MnO	2.37	2.73
otal	99.94	100.09	100.64	100.50	99.88	100.77		Total	100.31	100.43
	malized to 1								ormalized	
i ì	2.985 0.003	2.973 0.004	2.989 0.003	2.957 0.000	2.989 0.003	2.987 0.008		Si Ti	2.983 0.000	$\frac{2.991}{0.000}$
.l	1.975	1.997	1.959	2.015	1.968	1.970		Al	1.979	1.988
r	0.000	0.000	0.002	0.000	0.000	0.001		Cr	0.000	0.003
'e+++ 'e++	0.037 2.030	0.026 1.833	$0.046 \\ 1.800$	0.028 1.694	0.040 1.749	0.033 1.540		Fe*** Fe**	0.038 2.246	$0.018 \\ 1.982$
1g	0.307	0.301	0.155	0.364	0.235	0.223		Mg	0.395	0.604
Ca	0.523	0.736	0.670	0.656	0.713	0.738		Ca	0.226	0.244
⁄In	0.165	0.155	0.402	0.321	0.327	0.518		Mn	0.161	0.183
um	8.025	8.025	8.026	8.035	8.024	8.018		Sum	8.028	8.013
K Fe K Mg	$0.671 \\ 0.101$	0.606 0.100	0.595 0.051	$0.558 \\ 0.120$	$0.578 \\ 0.078$	0.510 0.074		X Fe X Mg	$0.742 \\ 0.130$	0.658 0.200
Ca Ca	0.101	0.100	0.031	0.120	0.236	0.244		X Ca	0.130	0.281
			0.122	0.106	0.108	0.172		X Mn	0.053	0.061
Mn	0.055	0.051	0.133	0.100	0.100	0.172		2 1 1 1 1 1 1 1	0.000	
	0.055	0.031	0.086	0.215	0.134	0.145		74 17411	3,322	
Mn			0.086							oclases_
( Mn (Mg/XFe	0.151	0.164	0.086	0.215	0.134	0.145			Plagi	
Mn			0.086	0.215				Sample Analysis #		oclases AS93241 A-27
Mn Mg/XFe	0.151 AS93126 J-98 42.02	0.164 AS93152 D-21 43.24	0.086 <b>Hornb</b> AS93204 B-19 41.89	0.215 <b>Dlendes</b> AS93221  D-20  43.09	0.134 AS93254 F-36 42.53	0.145 AS93274 A-7 42.45		Sample Analysis #	Plagi AS93159 I-3 60.39	AS93241 A-27 60.48
Mn (Mg/XFe ample nalysis # iO <sub>2</sub> iO <sub>2</sub>	0.151 AS93126 J-98 42.02 0.35	0.164 AS93152 D-21 43.24 0.63	0.086 <b>Hornb</b> AS93204  B-19  41.89  0.09	0.215 <b>Dendes</b> AS93221 D-20 43.09 0.61	0.134 AS93254 F-36 42.53 0.49	0.145 AS93274 A-7 42.45 0.45		Sample Analysis # SiO <sub>2</sub> Al <sub>2</sub> O <sub>3</sub>	Plagi AS93159 1-3 60.39 24.86	AS93241 A-27 60.48 24.63
AMn  AMg/XFe  ample nalysis #  iO <sub>2</sub> iO <sub>2</sub> cl <sub>2</sub> O <sub>3</sub>	0.151  AS93126 J-98  42.02 0.35 18.12	0.164 AS93152 D-21 43.24 0.63 14.98	0.086 <b>Hornb</b> AS93204  B-19  41.89  0.09  16.52	0.215 <b>Dlendes</b> AS93221  D-20  43.09  0.61  16.33	0.134 AS93254 F-36 42.53 0.49 16.98	0.145 AS93274 A-7 42.45 0.45 16.09		Sample Analysis # SiO <sub>2</sub> Al <sub>2</sub> O <sub>3</sub> CaO	Plagi AS93159 I-3 60.39 24.86 6.19	AS93241 A-27 60.48 24.63 5.61
Mn (Mg/XFe ample nalysis # iO <sub>2</sub> iO <sub>2</sub>	0.151  AS93126 J-98  42.02 0.35 18.12 16.94 7.29	0.164 AS93152 D-21 43.24 0.63 14.98 14.73 9.53	0.086  Hornh  AS93204  B-19  41.89  0.09  16.52  17.28  7.42	0.215 <b>Dendes</b> AS93221 D-20  43.09 0.61 16.33 14.28 9.73	AS93254 F-36 42.53 0.49 16.98 16.86 7.56	AS93274 A-7 42.45 0.45 16.09 16.64 8.38		Sample Analysis # SiO <sub>2</sub> Al <sub>2</sub> O <sub>3</sub> CaO Na <sub>2</sub> O K <sub>2</sub> O	Plagi AS93159 I-3 60.39 24.86 6.19 8.42 0.08	AS93241 A-27 60.48 24.63 5.61 8.28 0.04
ample nalysis # iO <sub>2</sub> cl <sub>2</sub> O <sub>3</sub> eO IgO	0.151  AS93126 J-98  42.02 0.35 18.12 16.94 7.29 0.18	0.164 AS93152 D-21 43.24 0.63 14.98 14.73 9.53 0.16	0.086  Hornb  AS93204  B-19  41.89 0.09 16.52 17.28 7.42 0.29	0.215 olendes AS93221 D-20 43.09 0.61 16.33 14.28 9.73 0.37	AS93254 F-36 42.53 0.49 16.98 16.86 7.56 0.24	AS93274 A-7 42.45 0.45 16.09 16.64 8.38 0.38		Sample Analysis # SiO <sub>2</sub> Al <sub>2</sub> O <sub>3</sub> CaO Na <sub>2</sub> O K <sub>2</sub> O FeO	Plagi AS93159 I-3 60.39 24.86 6.19 8.42 0.08 0.07	AS93241 A-27 60.48 24.63 5.61 8.28 0.04 0.31
ample nalysis # iO2 clo O3 eO O1 finO CaO	0.151  AS93126 J-98  42.02 0.35 18.12 16.94 7.29 0.18 11.02	0.164 AS93152 D-21 43.24 0.63 14.98 14.73 9.53 0.16 12.21	0.086  Hornb  AS93204  B-19  41.89 0.09 16.52 17.28 7.42 0.29 12.17	0.215 olendes AS93221 D-20 43.09 0.61 16.33 14.28 9.73 0.37 11.53	AS93254 F-36 42.53 0.49 16.98 16.86 7.56 0.24 11.44	AS93274 A-7 42.45 0.45 16.09 16.64 8.38 0.38 11.39		Sample Analysis # SiO <sub>2</sub> Al <sub>2</sub> O <sub>3</sub> CaO Na <sub>2</sub> O K <sub>2</sub> O	Plagi AS93159 I-3 60.39 24.86 6.19 8.42 0.08	AS93241 A-27 60.48 24.63 5.61 8.28 0.04
ample nalysis # iO2 ciO2 dl2O3 eO InO aO aO aO	0.151  AS93126 J-98  42.02 0.35 18.12 16.94 7.29 0.18 11.02 0.40	0.164 AS93152 D-21 43.24 0.63 14.98 14.73 9.53 0.16 12.21 0.64	0.086  Hornb  AS93204 B-19  41.89 0.09 16.52 17.28 7.42 0.29 12.17 0.36	0.215 AS93221 D-20 43.09 0.61 16.33 14.28 9.73 0.37 11.53 0.56	AS93254 F-36 42.53 0.49 16.98 16.86 7.56 0.24 11.44 0.53	AS93274 A-7 42.45 0.45 16.64 8.38 0.38 11.39 0.49		Sample Analysis # SiO <sub>2</sub> Al <sub>2</sub> O <sub>3</sub> CaO Na <sub>2</sub> O K <sub>2</sub> O FeO MgO	Plagi AS93159 1-3 60.39 24.86 6.19 8.42 0.08 0.07 0.00	AS93241 A-27 60.48 24.63 5.61 8.28 0.04 0.31 0.02
ample nalysis # iO2 clo O3 eO O1 finO CaO	0.151  AS93126 J-98  42.02 0.35 18.12 16.94 7.29 0.18 11.02	0.164 AS93152 D-21 43.24 0.63 14.98 14.73 9.53 0.16 12.21	0.086  Hornb  AS93204  B-19  41.89 0.09 16.52 17.28 7.42 0.29 12.17	0.215 olendes AS93221 D-20 43.09 0.61 16.33 14.28 9.73 0.37 11.53	AS93254 F-36 42.53 0.49 16.98 16.86 7.56 0.24 11.44	AS93274 A-7 42.45 0.45 16.09 16.64 8.38 0.38 11.39		Sample Analysis # SiO <sub>2</sub> Al <sub>2</sub> O <sub>3</sub> CaO Na <sub>2</sub> O K <sub>2</sub> O FeO	Plagi AS93159 I-3 60.39 24.86 6.19 8.42 0.08 0.07	AS93241 A-27 60.48 24.63 5.61 8.28 0.04 0.31
ample nalysis # iO2 iO2 clood fiO0 fio	AS93126 J-98 42.02 0.35 18.12 16.94 7.29 0.18 11.02 0.40 1.75	0.164  AS93152 D-21  43.24 0.63 14.98 14.73 9.53 0.16 12.21 0.64 1.40	0.086  Hornb  AS93204  B-19  41.89 0.09 16.52 17.28 7.42 0.29 12.17 0.36 1.33	0.215  AS93221 D-20  43.09 0.61 16.33 14.28 9.73 0.37 11.53 0.56 1.48	AS93254 F-36 42.53 0.49 16.98 16.86 7.56 0.24 11.44 0.53 1.22	AS93274 A-7 42.45 0.45 16.64 8.38 0.38 11.39 0.49 1.46		Sample Analysis # SiO <sub>2</sub> Al <sub>2</sub> O <sub>3</sub> CaO Na <sub>2</sub> O K <sub>2</sub> O FeO MgO	Plagi AS93159 1-3 60.39 24.86 6.19 8.42 0.08 0.07 0.00	AS93241 A-27 60.48 24.63 5.61 8.28 0.04 0.31 0.02
ample nalysis # iO2 clo2 clo3 eO InO laO	AS93126 J-98 42.02 0.35 18.12 16.94 7.29 0.18 11.02 0.40 1.75 0.11 98.19	AS93152 D-21 43.24 0.63 14.98 14.73 9.53 0.16 12.21 0.64 1.40 0.15 97.67	0.086  Hornb  AS93204 B-19  41.89 0.09 16.52 17.28 7.42 0.29 12.17 0.36 1.33 0.10 97.45	0.215  AS93221 D-20  43.09 0.61 16.33 14.28 9.73 0.37 11.53 0.56 1.48 0.10 98.08	AS93254 F-36 42.53 0.49 16.98 16.86 7.56 0.24 11.44 0.53 1.22 0.21 98.05	AS93274 A-7 42.45 0.45 16.64 8.38 0.38 11.39 0.49 1.46 0.14 97.87		Sample Analysis # SiO <sub>2</sub> Al <sub>2</sub> O <sub>3</sub> CaO Na <sub>2</sub> O K <sub>2</sub> O FeO MgO	Plagi AS93159 1-3 60.39 24.86 6.19 8.42 0.08 0.07 0.00	AS93241 A-27 60.48 24.63 5.61 8.28 0.04 0.31 0.02
ample malysis # GO2 ido Qo	AS93126 J-98 42.02 0.35 18.12 16.94 7.29 0.18 11.02 0.40 1.75 0.11 98.19 0.05	AS93152 D-21 43.24 0.63 14.98 14.73 9.53 0.16 12.21 0.64 1.40 0.15 97.67 0.06 97.60	0.086  Hornt  AS93204 B-19  41.89 0.09 16.52 17.28 7.42 0.29 12.17 0.36 1.33 0.10 97.45 0.04 97.40	0.215  AS93221 D-20  43.09 0.61 16.33 14.28 9.73 0.37 11.53 0.56 1.48 0.10 98.08 0.04	AS93254 F-36 42.53 0.49 16.98 16.86 7.56 0.24 11.44 0.53 1.22 0.21 98.05 0.09	AS93274 A-7 42.45 0.45 16.09 16.64 8.38 0.38 11.39 0.49 1.46 0.14 97.87 0.06		Sample Analysis # SiO <sub>2</sub> Al <sub>2</sub> O <sub>3</sub> CaO Na <sub>2</sub> O K <sub>2</sub> O FeO MgO Total	Plagi AS93159 I-3 60.39 24.86 6.19 8.42 0.08 0.07 0.00 100.00	AS93241 A-27 60.48 24.63 5.61 8.28 0.04 0.31 0.02 99.37
ample nalysis # iO2 clo2 digO finO laO la2 O la2 O la2 O late o l	0.151  AS93126 J-98  42.02 0.35 18.12 16.94 7.29 0.18 11.02 0.40 1.75 0.11 98.19 0.05 98.14  malized to 2 6.214	AS93152 D-21 43.24 0.63 14.98 14.73 9.53 0.16 12.21 0.64 1.40 0.15 97.67 0.06 97.60 3 equivale 6.399	0.086  Hornh  AS93204 B-19  41.89 0.09 16.52 17.28 7.42 0.29 12.17 0.36 1.33 0.10 97.45 0.04 97.40 nt O 6.280	0.215  Dendes  AS93221 D-20  43.09 0.61 16.33 14.28 9.73 0.37 11.53 0.56 1.48 0.10 98.08 0.04 98.04	AS93254 F-36 42.53 0.49 16.98 16.86 7.56 0.24 11.44 0.53 1.22 0.21 98.05 0.09 97.96	AS93274 A-7 42.45 0.45 16.09 16.64 8.38 0.38 11.39 0.49 1.46 0.14 97.87 0.06 97.81		Sample Analysis # SiO <sub>2</sub> Al <sub>2</sub> O <sub>3</sub> CaO Na <sub>2</sub> O K <sub>2</sub> O FeO MgO Total	AS93159 I-3 60.39 24.86 6.19 8.42 0.08 0.07 0.00 100.00	AS93241 A-27 60.48 24.63 5.61 8.28 0.04 0.31 0.02 99.37
ample nalysis #  iO2 clo 2 clo	0.151  AS93126 J-98  42.02 0.35 18.12 16.94 7.29 0.18 11.02 0.40 1.75 0.11 98.19 0.05 98.14  malized to 2 6.214 0.039	0.164  AS93152 D-21  43.24 0.63 14.98 14.73 9.53 0.16 12.21 0.64 1.40 0.15 97.67 0.06 97.60 3 equivale 6.399 0.070	0.086  Hornh  AS93204  B-19  41.89 0.09 16.52 17.28 7.42 0.29 12.17 0.36 1.33 0.10 97.45 0.04 97.40 nt O 6.280 0.010	0.215  AS93221 D-20  43.09 0.61 16.33 14.28 9.73 0.37 11.53 0.56 1.48 0.10 98.08 0.04 98.04	AS93254 F-36 42.53 0.49 16.98 16.96 7.56 0.24 11.44 0.53 1.22 0.21 98.05 0.09 97.96	AS93274 A-7 42.45 0.45 16.09 16.64 8.38 0.38 11.39 0.49 1.46 0.14 97.87 0.06 97.81 6.313 0.051		Sample Analysis # SiO <sub>2</sub> Al <sub>2</sub> O 3 CaO Na <sub>2</sub> O K <sub>2</sub> O FeO MgO Total  Cations no	Plagi AS93159 1-3 60.39 24.86 6.19 8.42 0.08 0.07 0.00 100.00	AS93241 A-27 60.48 24.63 5.61 8.28 0.04 0.31 0.02 99.37 to 8 oxyger 2.694 1.293
ample nalysis #  iO2 d2 d2O3 eO eO eO oT aO caO caO caO caO caO caO cao cao cations nor it	0.151  AS93126 J-98  42.02 0.35 18.12 16.94 7.29 0.18 11.02 0.40 1.75 0.11 98.19 0.05 98.14  malized to 2 6.214 0.039 3.157	0.164  AS93152 D-21  43.24 0.63 14.98 14.73 9.53 0.16 12.21 0.64 1.40 0.15 97.67 0.06 97.60 3 equivale 6.399 0.070 2.612	0.086  Hornh  AS93204  B-19  41.89 0.09 16.52 17.28 7.42 0.29 12.17 0.36 1.33 0.10 97.45 0.04 97.40  nt O 6.280 0.010 2.919	0.215  AS93221 D-20  43.09 0.61 16.33 14.28 9.73 0.37 11.53 0.56 1.48 0.10 98.08 0.04 98.04  6.3189 0.067 2.821	AS93254 F-36 42.53 0.49 16.98 16.86 7.56 0.24 11.44 0.53 1.22 0.21 98.05 0.09 97.96	AS93274 A-7 42.45 0.45 16.09 16.64 8.38 0.38 11.39 0.49 1.46 0.14 97.87 0.06 97.81		Sample Analysis # SiO <sub>2</sub> Al <sub>2</sub> O <sub>3</sub> CaO Na <sub>2</sub> O K <sub>2</sub> O FeO MgO Total  Cations no	Plagi  AS93159  I-3  60.39 24.86 6.19 8.42 0.08 0.07 0.00  100.00  ormalized ( 2.691 1.306 0.295	AS93241 A-27 60.48 24.63 5.61 8.28 0.04 0.31 0.02 99.37 to 8 oxygen 2.694 1.293 0.278
ample nalysis #  iO <sub>2</sub> d <sub>2</sub> O <sub>3</sub> eO fnO caO caO caO caC cations nor i i i i de	0.151  AS93126 J-98  42.02 0.35 18.12 16.94 7.29 0.18 11.02 0.40 1.75 0.11 98.19 0.05 98.14  malized to 2 6.214 0.039 3.157 2.095 1.606	0.164  AS93152 D-21  43.24 0.63 14.98 14.73 9.53 0.16 12.21 0.64 1.40 0.15 97.67 0.06 97.60 3 equivale 6.399 0.070 2.612 1.824 2.103	0.086  Hornt  AS93204  B-19  41.89 0.09 16.52 17.28 7.42 0.29 12.17 0.36 1.33 0.10 97.45 0.04 97.40  nt O  6.280 0.010 2.919 2.166 1.657	0.215  AS93221 D-20  43.09 0.61 16.33 14.28 9.73 0.37 11.53 0.56 1.48 0.10 98.08 0.04 98.04  6.3189 0.067 2.821 1.751	AS93254 F-36 42.53 0.49 16.98 16.86 7.56 0.24 11.44 0.53 1.22 0.21 98.05 0.09 97.96 6.305 0.055 2.966 2.090 1.669	AS93274 A-7 42.45 0.45 16.09 16.64 8.38 0.38 11.39 0.49 1.46 0.14 97.87 0.06 97.81 6.313 0.051 2.819 2.069		Sample Analysis # SiO <sub>2</sub> Al <sub>2</sub> O <sub>3</sub> CaO Na <sub>2</sub> O K <sub>2</sub> O FeO MgO Total  Cations no Si Al Ca Na K	Plagi AS93159 1-3 60.39 24.86 6.19 8.42 0.08 0.07 0.00 100.00	AS93241 A-27 60.48 24.63 5.61 8.28 0.04 0.31 0.02 99.37 to 8 oxyger 2.694 1.293 0.278 0.716 0.002
ample nalysis #  iO2 clood finO c	0.151  AS93126 J-98  42.02 0.35 18.12 16.94 7.29 0.18 11.02 0.40 1.75 0.11 98.19 0.05 98.14  malized to 2 6.214 0.039 3.157 2.095 1.606 0.023	0.164  AS93152 D-21  43.24 0.63 14.98 14.73 9.53 0.16 12.21 0.64 1.40 0.15 97.67 0.06 97.60 3 equivale 6.399 0.070 2.612 1.824 2.103 0.020	0.086  Hornh  AS93204 B-19  41.89 0.09 16.52 17.28 7.42 0.29 12.17 0.36 1.33 0.10 97.45 0.04 97.40 nt O 6.280 0.010 2.919 2.166 1.657 0.037	0.215  AS93221 D-20  43.09 0.61 16.33 14.28 9.73 0.37 11.53 0.56 1.48 0.10 98.08 0.04 98.04  6.3189 0.067 2.821 1.751 2.125 0.046	AS93254 F-36 42.53 0.49 16.86 7.56 0.24 11.44 0.53 1.22 0.21 98.05 0.09 97.96 6.305 0.055 2.966 2.090 1.669 0.030	AS93274 A-7 42.45 0.45 16.09 16.64 8.38 0.38 11.39 0.49 1.46 0.14 97.87 0.06 97.81 6.313 0.051 2.819 2.069 1.856 0.048		Sample Analysis # SiO <sub>2</sub> Al <sub>2</sub> O <sub>3</sub> CaO Na <sub>2</sub> O K <sub>2</sub> O FeO MgO Total  Cations no Si Al Ca Na K Mg	Plagi  AS93159 1-3 60.39 24.86 6.19 8.42 0.08 0.07 0.00  100.00  cormalized 0 2.691 1.306 0.295 0.728 0.005 0.000	AS93241 A-27 60.48 24.63 5.61 8.28 0.04 0.31 0.02 99.37 to 8 oxyger 2.694 1.293 0.278 0.716 0.002 0.001
ample malysis #  iO2 cla2O3 eeO la2O la2O la2O la2O lations nor icla latio	0.151  AS93126 J-98  42.02 0.35 18.12 16.94 7.29 0.18 11.02 0.40 1.75 0.11 98.19 0.05 98.14  malized to 2 6.214 0.039 3.157 2.095 1.606 0.023 1.746	0.164  AS93152 D-21  43.24 0.63 14.98 14.73 9.53 0.16 12.21 0.64 1.40 0.15 97.67 0.06 97.60 3 equivale 6.399 0.070 2.612 1.824 2.103 0.020 1.937	0.086  Hornh  AS93204  B-19  41.89 0.09 16.52 17.28 7.42 0.29 12.17 0.36 1.33 0.10  97.45 0.04 97.40  nt O 6.280 0.010 2.919 2.166 1.657 0.037 1.955	0.215  AS93221 D-20  43.09 0.61 16.33 14.28 9.73 0.37 11.53 0.56 1.48 0.10 98.08 0.04 98.04  6.3189 0.067 2.821 1.751 2.125 0.046 1.811	AS93254 F-36 42.53 0.49 16.98 16.86 7.56 0.24 11.44 0.53 1.22 0.21 98.05 0.09 97.96 6.305 0.055 2.966 2.090 1.669 0.030 1.817	AS93274 A-7 42.45 0.45 16.09 16.64 8.38 0.38 11.39 0.49 1.46 0.14 97.87 0.06 97.81 6.313 0.051 2.819 2.069 1.856 0.048 1.856		Sample Analysis # SiO <sub>2</sub> Al <sub>2</sub> O <sub>3</sub> CaO Na <sub>2</sub> O K <sub>2</sub> O FeO MgO Total  Cations no Si Al Ca Na K	Plagi  AS93159 1-3 60.39 24.86 6.19 8.42 0.08 0.07 0.00 100.00  ormalized 0 2.691 1.306 0.295 0.728 0.005	AS93241 A-27 60.48 24.63 5.61 8.28 0.04 0.31 0.02 99.37 to 8 oxyger 2.694 1.293 0.278 0.716 0.002
ample nallysis #  iO2 al2O aO aO aO aC	0.151  AS93126 J-98  42.02 0.35 18.12 16.94 7.29 0.18 11.02 0.40 1.75 0.11 98.19 0.05 98.14  malized to 2 6.214 0.039 3.157 2.095 1.606 0.023	0.164  AS93152 D-21  43.24 0.63 14.98 14.73 9.53 0.16 12.21 0.64 1.40 0.15 97.67 0.06 97.60 3 equivale 6.399 0.070 2.612 1.824 2.103 0.020	0.086  Hornh  AS93204 B-19  41.89 0.09 16.52 17.28 7.42 0.29 12.17 0.36 1.33 0.10 97.45 0.04 97.40 nt O 6.280 0.010 2.919 2.166 1.657 0.037	0.215  AS93221 D-20  43.09 0.61 16.33 14.28 9.73 0.37 11.53 0.56 1.48 0.10 98.08 0.04 98.04  6.3189 0.067 2.821 1.751 2.125 0.046	AS93254 F-36 42.53 0.49 16.86 7.56 0.24 11.44 0.53 1.22 0.21 98.05 0.09 97.96 6.305 0.055 2.966 2.090 1.669 0.030	AS93274 A-7 42.45 0.45 16.09 16.64 8.38 0.38 11.39 0.49 1.46 0.14 97.87 0.06 97.81 6.313 0.051 2.819 2.069 1.856 0.048		Sample Analysis # SiO <sub>2</sub> Al <sub>2</sub> O <sub>3</sub> CaO Na <sub>2</sub> O K <sub>2</sub> O FeO MgO Total  Cations no Si Al Ca Na K Mg	Plagi  AS93159 1-3 60.39 24.86 6.19 8.42 0.08 0.07 0.00  100.00  cormalized 0 2.691 1.306 0.295 0.728 0.005 0.000	AS93241 A-27 60.48 24.63 5.61 8.28 0.04 0.31 0.02 99.37 to 8 oxyge 2.694 1.293 0.278 0.716 0.002 0.001

Tab. A4 Results of garnet-biotite and garnet-hornblende thermometry, GASP barometry and analyses of plagioclases.

#### Garnet-biotite thermometry [°C] P = 5 kbar

AS93	106	116	126	136	137	152	159	179	204	205a	214	218	221	225	241	247	247b	252	254	259	260
N	60	27	42	19	9	13	48	27	32	18	18	8	15	27	54		25	21	28	24	12
Ferry and Spe	ar					100000															
mean temp std dev	360 7	386	470 14	572 19	577 32	516 30	548 20	552 14	365 12	523	425 14	592 66	545 14	585 20	540 27	-	545 18	552 8	484	516 26	592 62
Ganguly and	Saxena	ı	6																ļ	2	
mean temp std dev	439 8	497 25	502 12	609 18	636 35	563 35	546 18	553 13	436 14	514 9	502 12	582 61	576 13	597 17	502 18	-	580 17	589 7	528 16	506 24	621 57
Hodges and S	pear							3											ļ		
mean temp	443	517	530	631	683	608	578	572	440	541	500	630	624	623	571	-	584	593	546	545	621
std dev	8	24	15	19	35	34	20	13	15	10	11	66	15	21	28		17	7	11	26	66

# Garnet-hornblende thermometry [°C] P = 5 kbar

AS93	106	116	126	136	137	152	159	179	204	205a	214	218	221	225	241	247	247b	252	254	259	260
N			16			29		and colored a	43	1000		10234	9	OSS (Grove) - Kin		51	1850		53		.,,.
Graham and mean temp std dev	 Powell   -	-	578 20	-	-	574 12	-	_	528 38	-	-	_	595 6	-	-	583 15	-	-	582 22	-	-

# GASP barometry [kbar]

AS93	106	116	126	126	127	150	150	170	201	2050	214	210	221	225	241	247	2176	252	254	250	260
A393	100	110	120	130	137	134	137	1/7	204	ZUJa	214	210	441	223	241	241	24/0	ZJZ	234	239	200
															~ ~					5.7	
	a - 10-5	1.7		-	-	- 1	)			-	-			-	3-7	-		-	100	1 3-1	

# An % in plagioclase

AS93	106	116	126	136	137	152	159	179	204	205a	214	218	221	225	241	247	247b	252	254	259	260
	18	3-12	26-33	-	_	33-44	27-32		25-43	-			36-46	-	24-30	32-44	150			23-25	10 <del>-</del> 0

### Analytical technique

Mineral analyses were performed on the Cameca SX50 microprobe of the "Institut de Minéralogie et Pétrographie" of the Lausanne University. The following operating conditions were used: accelerating voltage: 15~kV; beam current: 20~nA for garnets, 15~nA for biotites and amphiboles, 10~nA for plagioclases; beam diameter: point mode for garnets, focused beam scanned on a  $4~by~6~\mu$  area for biotites and amphiboles, and on a  $5~by~7~\mu$  area for plagioclases.

### Garnet-biotite thermometry

Representative garnet and biotite analyses are given in Table A1. Garnet are normalized to 12 oxygens. Fe<sup>3+</sup> is estimated supposing that <sup>Y</sup>Fe<sup>3+</sup> = 2-(<sup>Y</sup>A1 + <sup>Y</sup>Cr + <sup>Y</sup>Ti). The Fe<sup>3+</sup> content is always very low and in most cases insignificant. Biotites were normalized to 22 equivalent oxygens. All the iron is considered to be bivalent. In each sample, contacts between garnets and biotites were preferred for temperature estimates. The rim of garnets is analysed and compared to the biotite analyzes located in the immediate vicinity. When textural equilibrium between garnets and biotites could not be found (i.e. AS 93152), the rim of garnet was used with the nearest biotite in the matrix.

Three calibrations (Ferry and Spear, 1978; Hodges and Spear, 1982; Ganguly and Saxena, 1984) were applied to each garnet-biotite assemblages (8 to 60 temperature estimates for one

calibration depending of the sample). The results are given in table A4. In addition, the Hodges and Spear's calibration results are plotted in histograms (Fig. 17). This provides a rapid and convenient way to judge the distribution and the coherence of the calculated temperatures. The temperatures considered as representative are printed in each histogram, and are compiled in figure 16c.

## Garnet-hornblende thermometry

The same philosophy is applied to the garnet-hornblende thermometry. Representative analyses are given in table A2. Hornblendes are normalized to 23 equivalent oxygens. Following the Graham and Powell (1984) calibration, all Fe is supposed to be bivalent. Results are given in table A4 as well as in histograms (Fig. 18).

# Garnet-Al<sub>2</sub>SiO<sub>5</sub>-quartz-plagioclase (GASP) geobarometer

Three samples (AS 93159, 241 and 259) contain the GASP geobarometer mineral assemblage. Pressures are calculated using the Hodges and Spear (1982) calibration. Representative analyses are given in table A3. Plagioclases are normalized to 8 oxygens. Intersection area between P-T lines for the GASP barometer and for the garnet-biotite geothermometer (both calibrations Hodges and Spear, 1982) are plotted in figure 19.